https://doi.org/10.5194/jecats-2026-13
Preprint. Discussion started: 28 July 2026
© Author(s) 2026. CC BY 4.0 License.

Can we achieve significant climate mitigation by optimising only for contrails?

Jakob Smretschnig[1], Feijia Yin[1], Dennis Piontek[2], Joël Clément[3], Sergio Núñez Arribas[3], Katrin Dahlmann[2], Federica Castino[1], and Volker Grewe[1,2]

[1]Delft University of Technology, Operations & Environment, Delft, The Netherlands
[2]Deutsches Zentrum für Luft- und Raumfahrt (DLR), Institut für Physik der Atmosphäre, Oberpfaffenhofen, Germany
[3]Thales AVS, Toulouse, France

Correspondence: Feijia Yin (F.Yin@tudelft.nl)

Abstract.

Contrail-avoidance is a widely studied measure to reduce the non-CO_2 climate effect of aviation. However, some mitigation gain is likely to be compromised through increased emissions (CO_2, NO_x, and H_2O) and their climate effect. Here, we analyse the impact of contrail-optimised flights on the overall net climate benefit. We evaluate more than 4,000 flights with large contrail impact traversing Northern Europe in 2023, each with two trajectory options: the filed trajectory submitted to the network manager and a contrail-optimised trajectory, allowing only vertical deviations and a maximum fuel penalty of 2%. Our model setup is based on the European Unions's non-CO_2 monitoring, reporting and verification (MRV) framework, modelling contrails with the contrail cirrus prediction model (CoCiP) and employing the algorithmic climate change functions (aCCFs) for NO_x and H_2O effects. This paper highlights three points: First, while 93% of contrail-optimised flights emit more NO_x (on average +2.5%), they emit it at lower, less climate-sensitive altitudes, so only 65% of flights exhibit an increased NO_x climate effect (+1.1%, measured in efficacy-weighted global warming potential over 100 years, $EGWP_{100}$), with considerable spatial and daily variability. Second, we find a risk of only 2% that the net climate benefit is not achieved when optimising for contrails alone, whereas using forecast weather data poses a far greater risk, causing optimisation to fail in ∼15% of cases. The net climate benefit, however, is reduced from -16.5% to -11.1%, measured in $EGWP_{100}$, when including NO_x and H_2O effects in the evaluation. Third, we find that the results are consistent to the choice of climate metric, with net climate benefit rates of -11.1%, -12.4%, and -16.2% obtained for $EGWP_{100}$, the average temperature response over 100 years (ATR_{100}), and $EGWP_{20}$, respectively. We conclude that savings attributed to contrail-avoidance under a hard constraint on extra fuel and considering flights with large contrail impact only, exceed the NO_x and H_2O penalties. We do, however, recommend further research that accounts for model uncertainties, in order to determine whether the clear dominance of contrail over NO_x (and H_2O) effects identified here for contrail-optimised trajectories remains robust.

1 Introduction

Aviation contributes to around 3.5–4.0% of the global anthropogenic warming through CO_2 and non-CO_2 emissions since 1940, when calculated in effective radiative forcing (ERF) for the year 2018 (Lee et al., 2021; Jaramillo et al., 2022). Consid-

https://doi.org/10.5194/jecats-2026-13
Preprint. Discussion started: 28 July 2026
© Author(s) 2026. CC BY 4.0 License.

ering the best estimates, the largest net warming is caused by contrail cirrus (57%), followed by CO_2 (34%) and NO_x (∼17%) (Lee et al., 2021). NO_x emissions at the upper troposphere and lower stratosphere leads to ozone (O_3) formation (warming) and methane (CH_4) destruction (net cooling), with ozone formation being about 2–3 times larger in magnitude (ERF), making it the driving force of the NO_x climate effect (Grewe et al., 2019; Lee et al., 2021; Szopa et al., 2021). The methane destruction also leads to a decrease in primary mode ozone (PMO) (Stevenson et al., 2004) and reduces stratospheric water vapour (Myhre et al., 2007). Other non-CO_2 effects include those caused by the emission of water vapour (H_2O), soot, and sulfate (IPCC, 1999; Wilcox et al., 2012; Lee et al., 2021).

While CO_2 emissions contribute to global warming regardless of when or where they occur, non-CO_2 effects behave non-linearly and are sensitive to the time and location of the emissions (Frömming et al., 2021; Maruhashi et al., 2022, 2024). Hence, numerous modelling studies have indicated that non-CO_2 effects can be significantly reduced through operational measures, particularly by optimising flight trajectories to avoid climate-sensitive regions (Matthes et al., 2012; Grewe et al., 2017; Matthes et al., 2020; Jaramillo et al., 2022). However, all studies applied only some uncertainty aspects, but did not investigate a full-range uncertainty. Most modelling studies are small-scale studies and only consider a single flight or a small number of flights, and few studies analyse air traffic on a larger scale (Simorgh et al. (2022), their Table 2 and 3; Simorgh and Soler (2025), their Table S1). Analysing a larger scale is relevant to capturing the conflicts that arise when multiple aircraft simultaneously adopt climate-optimal trajectories, since individually optimised trajectories can increase air traffic complexity and reduce the potential to resolve these conflicts. Such effects only become visible at network scale (Baneshi et al., 2023). Regardless of the number of flights analysed, the trajectory optimiser used, the climate effect addressed in the optimisation, or the climate metric chosen, all studies point to the same conclusion: substantial climate mitigation gains are achievable at little extra fuel cost.

Existing literature further demonstrates that only 2–6% of flights account for a share up to 80% of contrail warming for the air traffic they analysed (Teoh et al., 2020, 2024a; Piontek et al., 2026). That means deviating only flights with large contrail impact has already the potential to reduce the non-CO_2 effects substantially. Contrail avoidance is generally more straightforward than avoiding NO_x-sensitive regions. The regions of persistent contrails are usually characterized by sharp gradients due to their dependency on relative humidity with respect to ice, which varies quickly and on a daily basis. In contrast, NO_x sensitive regions are more depending on the general circulation and the transport pathway of the emitted species, e.g. advected towards the tropics or mid-latitudes (Rosanka et al., 2020). This leads to smooth gradients, which also show a seasonal pattern and dependency on how far away from the tropopause the NO_x was emitted (Frömming et al., 2021; Grewe and Stenke, 2008; Castino et al., 2024).

Trajectory optimisation can be achieved through either lateral or vertical flight path adjustments. Lührs et al. (2021) found that, for the same fuel penalty, reducing cruise altitude yields greater climate reductions than lateral deviation. Matthes et al. (2021) similarly compared flying permanently at lower versus higher altitudes, finding the same trend: a reduction of ∼33% versus an increase of ∼14% in non-CO_2 climate effect. More precisely, flying lower leads to a reduction of 11%, 18% and 26% in the contrail, NO_x and H_2O climate effect, respectively (Matthes et al. (2021), their Table 3). Another case study confirms the reduction of the NO_x climate effect when flying lower and slower (Zengerling et al., 2023). The authors further

https://doi.org/10.5194/jecats-2026-13
Preprint. Discussion started: 28 July 2026
© Author(s) 2026. CC BY 4.0 License.

show that contrails and NO_x contribute more to the total climate effect during summer, and CO_2 and H_2O during winter (their Fig. 7). However, considering contrails, this is in disagreement with results by Teoh et al. (2024a), who show a clear seasonal trend with contrail net RF peaking in winter and reaching its minimum in summer. While the trend of a reduced NO_x climate effect is similar for all three studies, they differ in their study setup from our work: Lührs et al. (2021) adjusts the trajectory continuously along its entire path, Matthes et al. (2021) uses a traffic inventory in which emissions are distributed continuously at lower altitudes, and Zengerling et al. (2023) investigated two sample flights and also reduced the speed of flights. Our approach introduces deviations at discrete air navigation fixes (waypoints) only (see Sect. 2.1), and we did not adjust the aircraft speed.

While previously mentioned results are based on modelling studies, Sausen et al. (2024) conducted the first operational tactical trial for contrail avoidance over multiple months in 2021 over airspaces in the Netherlands, Belgium, Luxembourg, Germany, and the North Sea. They were able to demonstrate that avoidance of persistent contrails is possible by air traffic management (ATM) for a small number of flight in non-peak times, however, the exact climate benefit is complex to quantify. Piontek et al. (2026) presented a fast-time simulation study on pre-tactical climate optimisation where 9% out of 145,000 flights were deviated vertically, based on historic weather data and applying a polygon-based climate optimisation approach. In polygon-based optimisation, polygons are created around climate-sensitive regions when a grid cell exceeds a predefined threshold. The optimiser then tries to avoid these regions completely, just like it would avoid an airspace with expected turbulence (Engberg et al., 2025). Kirschler et al. (2026) conducted a real world pre-tactical contrail avoidance trial of 25 commercial flights where they used weather forecasts and a cost-based climate optimisation approach to deviate flights vertically and laterally. In a cost-based optimisation, no threshold exists like in a polygon-based approach. Here, each grid cell is assigned a climate impact-related cost, and the optimiser tries to minimize the total cost when determining the trajectory. Engberg et al. (2025) demonstrated that cost-based optimisation reduced contrail-induced warming by 64%, while polygon-based optimisation achieved a 60% reduction. Within this study, we follow a cost-based optimisation that accounts for the climate effects of CO_2 and contrails.

To compare the climate effect of CO_2 and non-CO_2 emissions, a common climate metric has to be chosen. The non-CO_2 monitoring, reporting and verification (MRV) framework of the European Union suggests the usage of the efficacy-weighted global warming potential (EGWP) over 20, 50 or 100 years (European Commission, 2026; Grewe et al., 2026; Eichinger et al., 2025). Megill et al. (2024) tested various climate metrics against a set of requirements and came to the conclusion that the EGWP or the average temperature response (ATR) for a time horizon of at least 70 years is most suitable for representing the climate effect of aviation non-CO_2 emissions. Within this study, our baseline metric is the $EGWP_{100}$. We further evaluate the robustness of our results by comparing the $EGWP_{100}$ with the ATR_{100}, i.e. changing the climate metric. In addition, we also compare our results with the $EGWP_{20}$, i.e. changing the time horizon at which expected climate changes occur.

Lastly, one has to mention that modelling non-CO_2 effects is inherently uncertain, due to model limitations and the spread in results that arises when multiple models are applied under the same boundary conditions. This affects the robustness of contrail mitigation gain through operational measures (Lee et al., 2023; Grewe et al., 2026). To account for these uncertainties, several studies propose ways to address the associated risks (Prather et al., 2025; Grewe et al., 2026; Gierens, 2026; Borella

https://doi.org/10.5194/jecats-2026-13
Preprint. Discussion started: 28 July 2026
© Author(s) 2026. CC BY 4.0 License.

et al., 2026). Grewe et al. (2026), for instance, call for thorough validation and verification of the methods used, including consistency checks, rather than treating uncertainty as a reason for inaction. Smith et al. (2026) similarly points out that inaction is the largest climate risk.

In this study, we target flights with a large contrail impact and employ forecast weather data for optimisation and reanalysis data for evaluation to reflect the pre-tactical operational constraints. We follow a cost-based optimisation that accounts for the climate effects of CO_2 and contrails quantified in $EGWP_{100}$. The resulting trajectories are then evaluated against the full spectrum of non-CO_2 effects, including NO_x and H_2O emissions, using different climate metrics (efficacy-weighted GWP_{100}, ATR_{100}, and GWP_{20}). To the best of our knowledge, no prior study has examined how contrail-focused trajectory optimisation affects NO_x and H_2O climate impacts, nor whether the net climate mitigation benefit is preserved once these effects are accounted for. This study aims to address that gap.

The remaining paper is structured as follows: In Sect. 2, the used dataset is presented next to an overview of our model setup and the metric conversions. Then Sect. 3 describes the results of this study, answering specific research questions:

- **RQ1**: What impact does optimising for contrails have on the NO_x climate effect? (Sect. 3.2)
- **RQ2**: How much does the overall climate impact mitigation gain change when including NO_x and H_2O? (Sect. 3.3)
- **RQ3**: What impact does the climate metric choice have on the mitigation gain? (Sect. 3.4)

The results are further discussed in Sect. 4 before Sect. 5 draws conclusions of this study.

2 Data and methodology

2.1 Traffic data and trajectory optimisation

In this work, we analyse a subset of 4,112 flights selected from a broader dataset of around 150,000. The flights represent the ones with the largest contrail warming, which underwent trajectory rerouting (see Appendix A and Appendix B). The flights traverse airspaces managed by the Borealis alliance, a consortium of Northern European air navigation service providers (ANSPs) that implemented a free route airspace (Fig. 1). Of all flight segments, 29.4% lie within the Borealis airspace (accounting for a total of 5.7 million kilometres flown), with the remaining segments located in other airspaces. The flights were sampled on 16 systematically selected days in 2023 (see Sect. 2.4 in Piontek et al. (2026)) and cover 61 aircraft types.The number of flights with large contrail impact varies per day-pair: from 137 in June to 1083 in September (Fig. 1b). There is in general a significant share of long-haul flights, with short- and medium-haul flights together accounting for a similar proportion. The busiest airspaces are Shanwick, Ireland, Scotland and England, while Iceland, Bodø, Finland, Estonia and Latvia are rather quiet (Fig. 1c). The busiest day-pairs are 16 & 17 September 2023 and the day-pairs in December 2023, rather quiet are March and June 2023.

For each flight, two trajectory options are available in the dataset: the filed trajectory submitted to the network manager and the vertically adjusted contrail-mitigation trajectory. The contrail-optimised trajectories were generated based on HRES

https://doi.org/10.5194/jecats-2026-13
Preprint. Discussion started: 28 July 2026
© Author(s) 2026. CC BY 4.0 License.

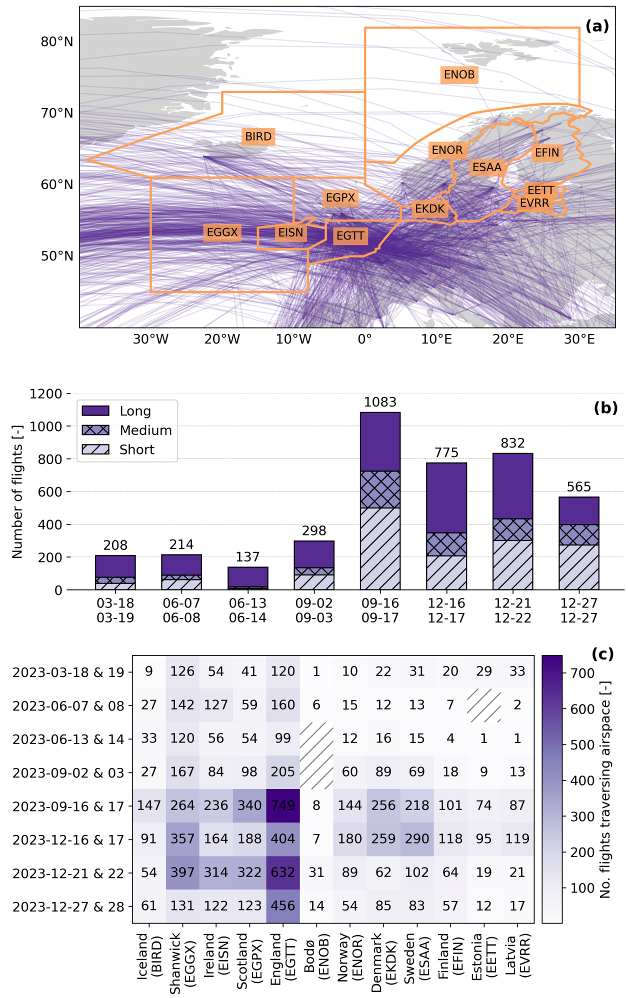

Figure 1. (a) Borealis airspaces (orange lines) and flight trajectories having large contrail impact (purple lines) in the dataset. (b) Number of flights having large contrail impact per day-pair in 2023 and haul type following the classification: up to 3 hours is a short-haul flight, up to 6 hours is a medium-haul flight, and beyond 6 hours is a long-haul flight. (c) Number of flights having large contrail impact crossing each airspace per day-pair. Note that one flight can cross multiple airspaces and therefore the sum of the rows is usually larger than the number of individual flights. Hatched boxes show airspaces with no flights on those days. Map in panel (a) made with cartopy and natural earth.

forecast data with lead times of 9–21 hours (see Appendix B). This decision was made because the lead time reflects operational constraints. Dean et al. (2025) further identified a reduction potential of contrail EF of 80–90% with lead times of 8–24 hours. Out of the original dataset with 4,112 flights, contrail avoidance is achieved for 88.2% of flights (lower contrail impact in the optimised trajectory, Δ Contrail < 0), while overall climate mitigation, accounting for both contrail and CO_2 (Δ $CO_2 +$ Δ Contrail < 0), is achieved for 85.2% of flights when evaluated with reanalysis data. The optimisation was carried out based on a cost-based approach with the objective of providing the most operations-oriented solution, which is essential for large

https://doi.org/10.5194/jecats-2026-13
Preprint. Discussion started: 28 July 2026
© Author(s) 2026. CC BY 4.0 License.

scale deployment. The operational point of view establishes acceptable limits and constraints imposed by the involved actors (network manager, ANSPs, and airspace users) with regards to the extra costs and benefits associated to the solution. The following operational constraints are enforced:

- Direct cost limits: Extra fuel is limited to less than 2% and extra flight time to less than 5 minutes relative to the filed flights.
- Minimum benefit threshold: Re-routing is only carried out if the potential climate benefit exceeds 5 $\mathrm{t(CO_{2eq})}$, $\mathrm{EGWP_{100}}$ with contrail efficacy of 0.42. The optimiser therefore proposes alternatives only to flights whose impact exceeds this threshold.
- Trajectory structure: Vertical deviations are permitted only within Borealis airspace, at most once per trajectory, and only at real-world air navigation fixes (waypoints), as required for flight plan management.
- Complexity at flow level: A complexity filter addresses the risk that too many flights are re-routed to lower flight levels, which could create excessive air traffic control (ATC) workload by increasing sector occupancy. Each optimised flight is assigned a *mitigation index* score reflecting the re-routing induced (in)convenience from an Air Traffic Flow and Capacity Management (ATFCM) perspective. Optimisations that would push ATFCM complexity beyond an acceptable limit are automatically removed, based on analysis of past sectorisation plans, capacity, and occupancy.

Within these constraints, vertical deviations take one of four forms: descent and climb again during cruise, delay the climb, descent early, or not fully climb at all (Fig. 2). These are all deviations which are in principle feasible for ATM operations and differ from the optimisation approach allowing continuous climb (Lührs et al., 2021) or constantly flying lower (Matthes et al., 2021).

The altitudes of the majority of flights (74.2%) deviate from the filed trajectories by 1000 to 8000 feet, with most deviating by 3000 to 4000 feet (30–40 FL) (Appendix C Fig. C1). This is comparable to the range of 1000 to 2000 feet for a fuel penalty of 2% that Lührs et al. (2021) report, and to the range of 0 to 6900 feet that Grewe et al. (2014a) report. Only the tactical flight trial by Sausen et al. (2024) limited the vertical deviation to 200 feet, but also considered a different airspace structure.

2.2 Model setup of evaluation

We follow the recommendations for the MRV by Eichinger et al. (2025). To evaluate the model setup, simulation results of aircraft performance, emissions, and climate effects were compared against literature data obtained under similar conditions (Sect. 3.1).

We use the aircraft performance model Base of Aircraft Data (BADA) 3.16 to estimate fuel flow (EUROCONTROL, 2022). BADA is a total energy model that provides a set of coefficients to calculate thrust, drag, engine efficiency and fuel flow during all phases of a mission. Nuic et al. (2010) report a mean error of less than 5% in the calculation of fuel consumption using BADA3. Version 3.16 supports 1,822 aircraft types, including the 61 aircraft from the dataset. We perform the fuel flow

https://doi.org/10.5194/jecats-2026-13
Preprint. Discussion started: 28 July 2026
© Author(s) 2026. CC BY 4.0 License.

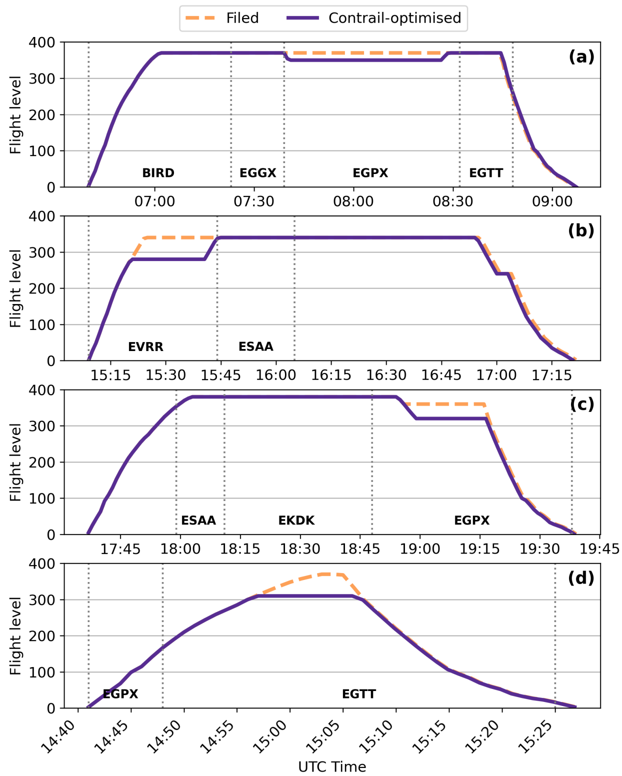

Figure 2. Illustrative examples of vertical profiles of the filed and contrail-optimised trajectories for four flights crossing different Borealis airspaces: (a) descent and climb during cruise-phase for flight BIKF–EHAM (A320neo), (b) late climb for flight EVRA–EBBR (A220), (c) early descent for flight EPGD–EGPH (A320), and (d) no full climb for flight EGAA–EGSS (A320neo).

calculation using BADA via the Python libraries pycontrails (version 0.54.11) and pycontrails-bada (version 0.7.7) (Shapiro et al., 2025).

To derive in-flight NO_x emissions, we apply the fuel flow method 2 (FFM2) (DuBois and Paynter, 2006), which extrapolates ground measurements of NO_x emissions from aircraft at four thrust settings from the ICAO emissions databank (EASA, 2025). This procedure indicates an uncertainty of about 10% when compared with measurements (DuBois and Paynter, 2006; Harlass et al., 2024).

In a similar way we calculate the in-flight non-volatile particulate matter (nvPM) emissions, both in mass and number. We apply the T4/T2 method developed by Teoh et al. (2022, 2024b) that extrapolates ground measurements of nvPM from the ICAO emissions databank (EASA, 2025) to cruise levels. The T4/T2 method has been compared with measurement data (Dischl et al., 2024) and estimates nvPM emissions with acceptable level of accuracy for the cruise phase. We calculate both NO_x and nvPM emissions using the pycontrails library (Shapiro et al., 2025).

https://doi.org/10.5194/jecats-2026-13
Preprint. Discussion started: 28 July 2026
© Author(s) 2026. CC BY 4.0 License.

We estimate the CO_2 emissions based on the calculated fuel flow, with a constant emission index of $EI_{CO_2} = 3.16\,\mathrm{kg(CO_2)\,kg(fuel)^{-1}}$ (ICAO, 2018). The take-off mass and the aircraft type are taken from the dataset and use the BADA default values.

For meteorological data, we use ERA5 reanalysis data from ECMWF (Copernicus Climate Change Service, 2018a, b), with an hourly temporal resolution and a spatial resolution of 0.25°× 0.25°, and pressure levels ranging from 1000 hPa to 150 hPa.

The ERA5 tropopause height, based on the WMO lapse-rate definition, is taken from Hoffmann and Spang (2021). The data is needed for the analysis of the NO_x and H_2O climate effects, which are linked to the tropopause height (IPCC, 1999; Castino et al., 2021; Frömming et al., 2021).

2.2.1 Contrail modelling

The contrail climate effect is calculated with pycontrails (version 0.54.11) (Shapiro et al., 2025), which is based on the contrail cirrus prediction model (CoCiP) (Schumann et al., 2012). CoCiP is a Lagrangian Gaussian plume model that simulates contrails over multiple hours for their climate effect. First, the Schmidt-Appleman criterion (SAC) (Schumann, 1996) is applied to determine whether or not a persistent contrail is formed. Then, the contrail wake vortex downwash is applied based on a parametrization, and the contrail width and depth are determined. Third, the ice water content and activated soot particles are calculated based on the emitted nvPM, to determine the ice crystals. From here on, the contrail evolution (including advection, lifetime, and micro-, macro- and optical properties) is simulated, considering wind shear and sedimentation. The instantaneous radiative forcing is estimated based on a parametrization of a comprehensive radiative transfer model. Lastly, the radiative forcing (RF) is estimated for both long wave and short wave radiation, to then determine the simulation output in energy forcing (EF, in J) as in

$$EF_{contrail}[J] = \int_{0}^{t_{max}} RF'_{net}(t) \times L(t) \times W(t)dt \tag{1}$$

with the instantaneous net radiation change RF'_{net} (in $\mathrm{W\,m^{-2}}$), the contrail lifetime t_{max} (in s), and the segment length and width of the contrail L (in m) and W (in m), respectively. CoCiP has been verified against in-situ measurements from flight campaigns (Schumann et al., 2017; Voigt et al., 2022; Harlass et al., 2024; Märkl et al., 2024) and ground-based remote sensing (Low et al., 2025). In this study, we configure pycontrails with 12 h maximum contrail age (which is a conservative estimate, since most contrails dissolve after a few hours), 10 minutes time integration (as a reasonable compromise between temporal resolution and computational cost), and humidity scaling according to Teoh et al. (2022) (to correct the underestimation of ice-supersaturation in ERA5 data). This is in line with recommendations by the MRV as well (Eichinger et al., 2025).

2.2.2 NO_x and H_2O climate effect modelling

The climate effects of NO_x-related O_3 and CH_4 as well as H_2O are calculated using the algorithmic climate change functions (aCCFs) (Van Manen and Grewe, 2019; Yin et al., 2023; Dietmüller et al., 2023), as also recommended for the MRV (Eichinger et al., 2025). aCCFs are based on climate change functions (CCFs) developed by Grewe et al. (2014b), that describe the

https://doi.org/10.5194/jecats-2026-13
Preprint. Discussion started: 28 July 2026
© Author(s) 2026. CC BY 4.0 License.

estimated climate effect of an emission at a certain location and time considering a specific weather situation. CCFs were originally developed for five representative winter and three representative summer weather patterns over the North-Atlantic corridor (Irvine et al., 2013; Frömming et al., 2021). Rosanka et al. (2020) and Frömming et al. (2021) showed that the impact of an emission of NO_x as well as H_2O has a clear dependency on the weather pattern, in which the emission occurs. For NO_x, e.g., the initial transport pathway largely controls the strength and duration of the main ozone signal. Van Manen and Grewe (2019) used this finding and approximated the eight CCFs through a regression analysis and created the aCCFs, a computationally efficient model that relies solely on meteorological inputs such as temperature, potential vorticity, and geopotential. Based on the similarity of the transport pathways, the authors claim that the aCCFs can be applied to the northern hemisphere for 30–60° N. In general this has been shown by Maruhashi et al. (2022), however, one should still be cautious in their usage since the adjusted regression coefficient R^2 of below 0.5 for the NO_x components ozone and methane indicates that the regression explains less than half of the variance in the data, and thus, their accuracy is limited. Later work by Dietmüller et al. (2023) highlights important seasonal and regional limitations to consider as well. The NO_x-O_3 aCCFs were evaluated by including the aCCFs in an EMAC simulation that allows an aircraft trajectory optimisation (Yamashita et al., 2020; Yin et al., 2018b). The results show that those NO_x-O_3 aCCF-optimised trajectories reduce the ozone radiative forcing for both lateral and vertical re-routing (Rao et al., 2022; Yin et al., 2023). Although a basic verification was performed (see above), a proper validation of (a)CCFs against observational data is not feasible (Grewe et al., 2014b).

In this work, we use the aCCFs in their version 1.0A (Matthes et al., 2023), and consider a pulse emission scenario. Version 1.0A was chosen as Matthes et al. (2023) aligned the individual climate effects of aCCFs with the climate response model AirClim (Grewe and Stenke, 2008; Dahlmann et al., 2016), yielding in aligned absolute values which are relevant for this study to quantify the potential trade-off between CO_2, contrails, NO_x and H_2O. In the original set of aCCFs, the emphasis was on the temporal and spatial gradients of non-CO_2 effects, so that aCCFs could be used as objective functions to identify trajectories minimising climate impact. Maruhashi et al. (2024) showed that the CCF modelling approach for NO_x-O_3 and thereby the aCCFs well describe the sensitivities of the more detailed EMAC model, however an offset was identified. Therefore the alignment of the aCCFs to AirClim ensures that the climate effect from annual air traffic is reproduced, while maintaining the sensitivities from the detailed EMAC model. A review of the three different aCCF versions is given in Table 1, and the scaling factors to get from one aCCF version to the other are shown in Appendix D.

Furthermore, the validity range of the aCCFs was set to 150-350 hPa. Outside these boundaries the aCCFs and thus, the quantified climate effect, is set to zero. The original CCFs were based on standardized emissions at pressure levels 200, 250, 300, and 400 hPa (Frömming et al., 2021). Whether extrapolation beyond this range is valid remains unknown. However, since 25.9% of all flights in this study have filed flight segments at pressure levels <200 hPa (i.e. flying higher; see Appendix C Fig. C1), we decided to extrapolate towards 150 hPa. This is taken into consideration in the evaluation. Looking at the other side of the range, CCFs and aCCFs for ozone show a different trend between 350 to 400 hPa (Van Manen and Grewe (2019), their Fig. 8), mainly due to the conversion from RF to adjusted RF. With new aCCF versions in the pipeline based on work by Maruhashi et al. (2022, 2024); Rao et al. (2024); Frömming et al. (2026), this inconsistency would likely be eliminated. However, for now we decided to exclude the pressure level 400 hPa from our validity range. In addition, whenever

https://doi.org/10.5194/jecats-2026-13
Preprint. Discussion started: 28 July 2026
© Author(s) 2026. CC BY 4.0 License.

aCCF version	Species	Characteristics
Van Manen and Grewe (2019)	O_3, CH_4, H_2O	Original version, directly derived from CCF output. Shows a good representation of the mechanism, and follows the climate response function of Boucher and Reddy (2008).
Yin et al. (2023) and Dietmüller et al. (2023)	O_3, CH_4, H_2O, Contrails, CO_2	First complete set of aCCFs based on consistent pulse emission scenario, following the climate response function of Sausen and Schumann (2000).
Matthes et al. (2023)	O_3, CH_4, H_2O, Contrails, CO_2	Absolute values are aligned with AirClim (Grewe and Stenke, 2008; Dahlmann et al., 2016) using alignment factors. Follows the climate response function of Sausen and Schumann (2000).

Table 1. Characteristics of the three different algorithmic climate change function (aCCF) versions. In this work we use the aCCFs by Matthes et al. (2023).

an optimised flight segment falls outside the validity range, its corresponding (unoptimised) segment is also excluded entirely from the evaluation. This is required since the delta would otherwise always equal the climate effect of the filed flight segments and hence, over/underestimate the real change (Appendix C Fig. C2).

To improve computational performance, we run CoCiP and the aCCF calculation and interpolation along the trajectory waypoints on the DelftBlue supercomputer (DHCP, 2024). Thereby, we divide the full set of flights into eight day-pairs of 48 h, and also separate between filed and contrail-optimised trajectories. We further parallelize the CoCiP calculation using 12 tasks via the message passing interface (MPI), dividing the flights within the 48 h groups into 12 subsets, each processed independently (Rogowski et al., 2023).

2.3 Climate metric conversions

To compare the climate effect of CO_2 emissions, contrails, and NO_x and H_2O emissions, different model outputs must be converted to a common climate metric. The climate metric is a combination of emission scenario (e.g. pulse (P), business-as-usual (BAU)), climate indicator (e.g. efficacy-weighted absolute GWP (EAGWP), average temperature response (ATR)), and time horizon (e.g. 20, 100). In this work, all emission scenarios are pulse emissions (prefix P). For clarity, we only use the prefix in this section and omit it elsewhere. We follow the approach by Piontek et al. (2026) (their Appendix) to convert climate metrics using conversion factors κ from Dahlmann et al. (2025) (their Table 3). The relevant subset of these factors is listed in Table 2, where $\kappa_{r,c}$ denotes the entry in row r (climate metric) and column c (species).

Drawing on factors $\kappa_{r,c}$ from Dahlmann et al. (2025), we define $f_{i\to j}(x)$ as the conversion factor that describes the conversion from climate metric i to j for any species x:

$$f_{i\to j}(x) = \frac{\kappa_{j,x}}{\kappa_{i,x}} \tag{2}$$

https://doi.org/10.5194/jecats-2026-13
Preprint. Discussion started: 28 July 2026
© Author(s) 2026. CC BY 4.0 License.

κ	CO_2	H_2O	O_3	CH_4	Contrail
P-EAGWP$_{100}$	46.5486	1.0192	1.0702	13.8903	0.2100
P-EAGWP$_{20}$	15.1263	1.0192	1.0702	11.0517	0.2100
P-ATR$_{100}$	0.3223	0.0078	0.0082	0.1059	0.0016
P-ATR$_{20}$	0.3481	0.0320	0.0337	0.2838	0.0065

Table 2. Conversion from RF to other climate indicators and time horizons for pulse emissions (P2025), from Dahlmann et al. (2025) (their Table 3). The units are year for AGWP and K $(\mathrm{W\ m^{-2}})^{-1}$ for ATR.

Parameter	Value	Reference
CO_2	1.00	-
O_3	1.05	Ponater (2010)
CH_4	1.04	Ponater (2010)
Contrail (optimisation)	0.42	Lee et al. (2021)
Contrail (evaluation)	0.21	Bickel et al. (2025)
H_2O	1.00	-

Table 3. Efficacies used in this study. Aligned with Dahlmann et al. (2025) to be best compatible with the conversion factors in Table 2.

Our goal is to derive the climate effects from all four species (CO_2, Contrails, NO_x, H_2O) in three metrics: P-EGWP$_{100}$, P-ATR$_{100}$, and P-EGWP$_{20}$, all in $\mathrm{tCO_{2}}_{eq}$. To account for the differences of each species in impacting the global near surface temperature, we consistently apply the set of efficacies listed in Table 3. Note that the P-AGWP is equal to the P-EAGWP for CO_2, as the efficacy for CO_2 by definition is 1.0.

2.3.1 Climate effect of CO_2 emissions

The CO_2 climate effect is either directly given in $\mathrm{tCO_2}$ or converted into a temperature response in K depending on the metrics used. The temperature is calculated by multiplying the mass of CO_2 with best estimates of the specific ($spec$) P-AGWP$^{spec}_{TH}$(CO_2) by Gaillot et al. (2023) and further multiplying with the conversion factors by Dahlmann et al. (2025). The P-AGWP$^{spec}_{TH}$(CO_2) estimates for time horizons TH of 100 and 20 years are:

$$P\text{-}AGWP^{spec}_{100}(\mathrm{CO_2}) = 8.80\times10^{-14}\ \mathrm{W\ m^{-2}\ yr\ kg(CO_2)^{-1}} \tag{3}$$

$$P\text{-}AGWP^{spec}_{20}(\mathrm{CO_2}) = 2.39\times10^{-14}\ \mathrm{W\ m^{-2}\ yr\ kg(CO_2)^{-1}} \tag{4}$$

To derive the P-ATR$_{100}$ for CO_2, we use:

$$P\text{-}ATR_{100}(\mathrm{CO_2}) = m_{\mathrm{CO_2}} \times P\text{-}AGWP^{spec}_{100}(\mathrm{CO_2}) \times f_{P\text{-}AGWP_{100}\rightarrow P\text{-}ATR_{100}}(\mathrm{CO_2}) \tag{5}$$

https://doi.org/10.5194/jecats-2026-13
Preprint. Discussion started: 28 July 2026
© Author(s) 2026. CC BY 4.0 License.

2.3.2 CO_{2eq} emissions

The principle to calculate the CO_{2eq} emissions in kg based on the P-EAGWP metric for species x and time horizon TH is:

$$CO_{2eq} = \frac{P\text{-}EAGWP_{TH}(x)}{P\text{-}AGWP_{TH}^{spec}(\mathrm{CO_2})} \tag{6}$$

Note that we use the definition of the *specific* AGWP of CO_2 by Gaillot et al. (2023), $P\text{-}AGWP_{TH}^{spec}(\mathrm{CO_2})$, that defines the climate response of CO_2 explicitly per unit mass emitted. Hence, this division directly yields $\mathrm{kg(CO_{2eq})}$ emissions and is independent of the fuel used (e.g. kerosene, sustainable aviation fuel (SAF), hydrogen).

Alternatively, the average temperature response (ATR) can be determined with the conversion factors for species x and time horizon TH:

$$P\text{-}ATR_{TH}(x) = P\text{-}EAGWP_{TH}(x) \times f_{P\text{-}EAGWP_{TH} \rightarrow P\text{-}ATR_{TH}}(x) \tag{7}$$

Also the ATR can then be converted to CO_{2eq} using the climate effect per $\mathrm{kg(CO_2)}$ P-ATR$_{TH}^{spec}(\mathrm{CO_2})$ from Dahlmann et al. (2025) (their Table 6):

$$CO_{2eq} = \frac{P\text{-}ATR_{TH}(x)}{P\text{-}ATR_{TH}^{spec}(\mathrm{CO_2})} \tag{8}$$

The default output of the contrail model CoCiP is energy focing (EF), which is measured in J. The P-EAGWP for contrails, given in $\mathrm{W\,m^{-2}\,yr}$, is defined as

$$P\text{-}EAGWP_{\text{contrail}} = \frac{EF_{\text{contrail}}}{S_{\text{earth}} \times t_{\text{seconds per year}}} \times r_{RF} \tag{9}$$

EF_{contrail} is the CoCiP output in J, and all other variables are constants: S_{earth} is the surface area of the Earth in $\mathrm{m^2}$ and $t_{\text{seconds per year}}$ are the seconds per year in s. Hence the first factor is equivalent to the RF and the second factor is the contrail efficacy calculated on the basis of RF, $r_{\text{contrail}} = 0.21$ (Bickel et al., 2025), which is unitless, to be also aligned with the conversion factors.

The default output of aCCFs is the ATR over 20 years in K per emitted NO_2 or burned fuel, assuming a pulse emission (P-ATR$_{20}$). For the O_3 and CH_4 aCCFs, the units are $\mathrm{K\,kg(NO_2)^{-1}}$, and the H_2O aCCF is given in $\mathrm{K\,kg(fuel)^{-1}}$. Following standard aviation emissions practice (ICAO, 2016; Lee et al., 2023), NO_x is reported in NO_2-equivalent units, since NO rapidly oxidizes to NO_2 after emission. The P-ATR$_{20}$ (in K) can be easily determined by multiplying the aCCF with the NO_x mass or fuel mass, respectively. To convert the P-ATR$_{20}$ into any other metric, for instance into the P-EAGWP$_{100}$, the conversion factor $f_{i \rightarrow j}(x)$ can be applied again (see Eq. 2). Note that the conversion factors by Dahlmann et al. (2025) are only valid under a consistent Boucher and Reddy (2008) climate response function. Whenever another parametrisation is used, as is the case for two aCCF versions (see Table 1), the corresponding backward calculation factors β_x (Appendix D Table D2) for species x must be introduced as divisors to account for this discrepancy.

https://doi.org/10.5194/jecats-2026-13
Preprint. Discussion started: 28 July 2026
© Author(s) 2026. CC BY 4.0 License.

The P-EAGWPs can then be calculated for all respective aCCFs using:

$$P\text{-}EAGWP_{100}(\mathrm{H_2O}) = \mathrm{aCCF_{H_2O}} \times \beta^{-1}_{\mathrm{H_2O}} \times m_f \times r_{\mathrm{H_2O}} \times f_{P\text{-}ATR_{20} \rightarrow P\text{-}EAGWP_{100}}(\mathrm{H_2O}) \tag{10}$$

$$P\text{-}EAGWP_{100}(\mathrm{O_3}) = \mathrm{aCCF_{O_3}} \times \beta^{-1}_{\mathrm{O_3}} \times \mathrm{EI_{NO_x}} \times m_f \times r_{\mathrm{O_3}} \times f_{P\text{-}ATR_{20} \rightarrow P\text{-}EAGWP_{100}}(\mathrm{O_3}) \tag{11}$$

$$P\text{-}EAGWP_{100}(\mathrm{CH_4}) = \mathrm{aCCF_{CH_4}} \times \beta^{-1}_{\mathrm{CH_4}} \times \mathrm{EI_{NO_x}} \times m_f \times r_{\mathrm{CH_4}} \times f_{P\text{-}ATR_{20} \rightarrow P\text{-}EAGWP_{100}}(\mathrm{CH_4}) \tag{12}$$

with $\mathrm{aCCF_{H_2O}}$ in K kg(fuel)$^{-1}$ and $\mathrm{aCCF_{O_3}}$ and $\mathrm{aCCF_{CH_4}}$ in K kg(NO_2)$^{-1}$. Furthermore, β_x is the dimensionless backward calculation factor, m_f is given in kg(fuel), $\mathrm{EI_{NO_x}}$ in kg(NO_2) kg(fuel)$^{-1}$, r is the unitless efficacy (see Table 3), and $f_{i \rightarrow j}(x)$ is given in W m^{-2} yr K^{-1}.

Note that the aCCFs are computed on a 4D grid (latitude, longitude, altitude, time), then spatially and temporally interpolated to the aircraft's flight trajectory, and then summed along the trajectory to obtain the aggregated sum. From here onwards, Eq. (6) can be used to derive CO_{2eq} values, or Eq. (7) can be used to derive a temperature response.

3 Results

3.1 Fuel burn, emissions, and climate effect

With the model chain described in Sect. 2, we calculate the fuel burn, CO_2, NO_x and nvPM emissions, and the climate effect of contrails, NO_x, and H_2O for the contrail-optimised flights. Accordingly, contrail-optimal routing with vertical trajectory adjustments increases fuel use and CO_2 emissions by 1.2%, NO_x emissions by 2.5%, nvPM emissions by 2.1–2.8%, the NO_x climate effect by 1.1%, while reducing contrails by 43.5% and the H_2O climate effect by 1.2% (Table 4). To check the consistency of the implementation, we compare our results against regional references where available, and global estimates otherwise. The regional reference by Piontek et al. (2026) considers the same sample days and Borealis region as our study, but a total of around 145,000 flights compared to our sample of approximately 4,000 flights with large contrail impact. The global reference by Teoh et al. (2024b) presents annual mean values of 2019 derived from 40 million unoptimised flights. Thus, it should be noted that the comparison is only an approximation. Our distance-normalised fuel burn estimates with BADA3 are within the range of the regional reference, but larger than the global reference. Besides the comparison with a global annual mean, the fuel burn discrepancy to the global reference may further be attributed to the fact that their data rely on a combination of the BADA3 and BADA4 aircraft performance models. The CO_2 estimates per distance fall within the range of the regional reference, though toward the upper bound. Our distance-normalised NO_x emission estimates with FFM2, and our nvPM mass and number emission estimates with the T4T2 method are all larger than the global reference. Same accounts for the contrail EF per distance. The normalised NO_x climate effect is within the range of the regional reference. This holds despite the fact that our CO_{2eq} values are based on the $\mathrm{EGWP_{100}}$, which incorporates the efficacies of O_3 and CH_4 (see Table 3), whereas the other authors employ the $\mathrm{GWP_{100}}$. Given that the efficacies for ozone and methane are close to unity, excluding them from our results would still leave our results within their reported range.

https://doi.org/10.5194/jecats-2026-13
Preprint. Discussion started: 28 July 2026
© Author(s) 2026. CC BY 4.0 License.

Variable	Filed	Optimised	Δ (%)	Global reference[1]	Regional reference[2]
Distance travelled ($\times10^6$ km)	19.5	19.5	0%*		
Fuel burn (Gg)	123.0	124.5	+1.2 %		
Fuel burn per distance (kg km^{-1})	6.3	6.4	+1.2 %	4.7	3.0–8.4
CO_2 (Gg)	388.6	393.2	+1.2 %		
CO_2 per distance (kg km^{-1})	19.9	20.2	+1.2 %	14.5	8.3–20.1
Mean EI NO_x (g kg^{-1})	14.6	14.7	+1.0 %		
NO_x (as NO_2, Mg)	2.06	2.11	+2.5 %		
NO_x per distance (as NO_2, kg(NO_2) km^{-1})	0.106	0.108	+2.5 %	0.074	
Mean nvPM EI_m (g kg^{-1})	0.073	0.073	+0.3 %		
Mean nvPM EI_n ($\times10^{15}$ kg^{-1})	1.104	1.115	+1.0 %		
nvPM mass (kg)	7,728	7,892	+2.1 %		
nvPM number ($\times10^{22}$)	9.55	9.81	+2.8 %		
nvPM mass per distance (g km^{-1})	0.396	0.405	+2.1 %	0.351	
nvPM number per distance ($\times10^{15}$ km^{-1})	4.897	5.032	+2.8 %	4.644	
$EF_{contrail}$ ($\times10^{18}$ J)	1.717	0.970	-43.5 %		
Contrail effect (Gg(CO_{2eq}), $EGWP_{100}$)	254.5	143.7	-43.5 %		
$EF_{contrail}$ per distance ($\times10^{10}$ J km^{-1})	8.805	4.974	-43.5 %	1.64	
Contrail per distance (kg(CO_{2eq}) km^{-1})	13.1	7.4	-43.5 %		
NO_x effect (Gg(CO_{2eq}), $EGWP_{100}$)	266.3	269.3	+1.1 %		
NO_x per distance (kg(CO_{2eq}) km^{-1})	13.7	13.8	+1.1 %		5.3 [0.2, 19]
NO_x per distance (long) (kg(CO_{2eq}) km^{-1})	15.9	16.1	+1.2 %		14.7 [0.4, 19]
NO_x per distance (medium) (kg(CO_{2eq}) km^{-1})	4.3	4.4	+0.8 %		4.2 [0.2, 7]
NO_x per distance (short) (kg(CO_{2eq}) km^{-1})	3.2	3.3	+0.7 %		2.3 [0.2, 4]
H_2O effect (Gg(CO_{2eq}), $EGWP_{100}$)	21.8	21.6	-1.2 %		
H_2O per distance (kg(CO_{2eq}) km^{-1})	1.119	1.106	-1.2 %		

Table 4. Simulation results such as distance travelled, fuel burn, NO_x and nvPM emissions, and contrail climate effect for the whole mission for filed and contrail-optimised trajectories. Climate effect values for NO_x and H_2O only represent the cruise phase due to model limitations. The climate metric considered is the $EGWP_{100}$. Normalised delta values are compared to literature. Haul-type classifications are based on distance: <1,500 km (short), 1,500–4,000 km (medium), >4,000 km (long). *Due to the vertical only adjustments of flights and the geodesic distance calculation, no change occurs. [1]Teoh et al. (2024a, b), [2]Piontek et al. (2026).

https://doi.org/10.5194/jecats-2026-13
Preprint. Discussion started: 28 July 2026
© Author(s) 2026. CC BY 4.0 License.

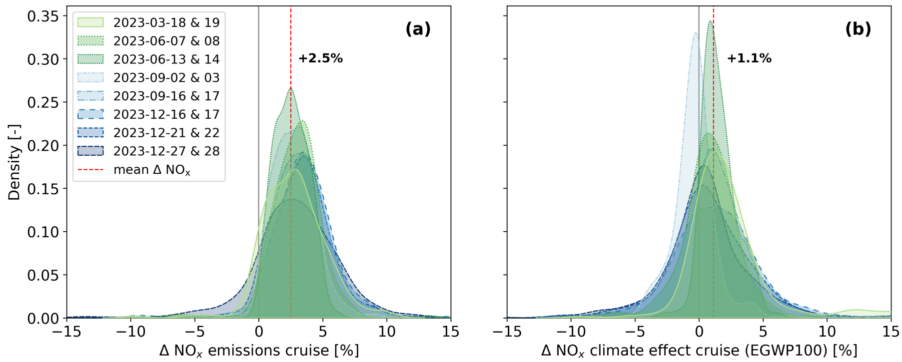

Figure 3. Distribution of relative change in NO_x emissions (a) and NO_x climate effect in $EGWP_{100}$ (b) per individual flight after contrail-optimisation.

3.2 What impact does optimising for contrails have on the NO_x climate effect?

Our results (Fig. 3) show that contrail-optimised flights emit on average +2.5% NO_x (cruise only), whereas the NO_x climate effect ($EGWP_{100}$) only increases by +1.1%. This relates to 93% of contrail-optimised flights that emit more NO_x, but only 65% of contrail-optimised flights exhibit an increased NO_x climate effect. Zooming into individual day-pairs (Fig. 4a), these fractions show large temporal variability: on 13 & 14 June 2023, 99% of contrail-optimised flights exhibit higher NO_x emissions than before, and 94% also show an increased NO_x climate effect. This indicates a strong correlation between NO_x emissions and its climate effect on these days. On 2 & 3 September 2023, however, 99% of flights have higher NO_x emissions, but only 37% of flights have a higher NO_x climate effect. That is due to the small vertical adjustments of the trajectories on that day pair (Fig. 4b). While the average temporal vertical detour across all flights is approximately -5500 ft, it was only -3100 ft on this day pair. For the sensitivity of the results to changes in the vertical extent over which the aCCF model is considered valid, we refer you to Fig. C3.

Furthermore, we find considerable spatial variability in the changes in NO_x emissions, as well as in the NO_x climate effect. This is illustrated in Fig. 5. For the vast majority of airspaces and day-pairs, the NO_x emissions are increased (see panel (a)). Most consistently are the increases over the Shanwick airspace, ranging from 3–10%, whereas all other airspaces show larger variability. The NO_x climate effect is also higher for most airspaces and day-pairs, however, not for all of them, and it sometimes even changes sign (see panel (b)). For example, the two Norwegian airspaces (Bodø, Norway) show a decrease of 2–7% in the NO_x climate effect for the last two December day-pairs, despite an increase of 4–13% in NO_x emissions. Normalising the change in climate effect by the change in emission (panel (c)) gives the additional climate effect per kilogram of extra NO_x emitted. Most consistently here is the day-pair 16 & 17 September 2023, with an additional climate effect of 53–121 $\mathrm{kg(CO_{2eq})\ kg(NO_x)^{-1}}$.

To understand what drives the divergence between NO_x emissions and climate effect, we consider another example. Figure 6 shows a comparison of the two day-pairs 16 & 17 December and 21 & 22 December within seven airspaces (Bodø, Norway,

https://doi.org/10.5194/jecats-2026-13
Preprint. Discussion started: 28 July 2026
© Author(s) 2026. CC BY 4.0 License.

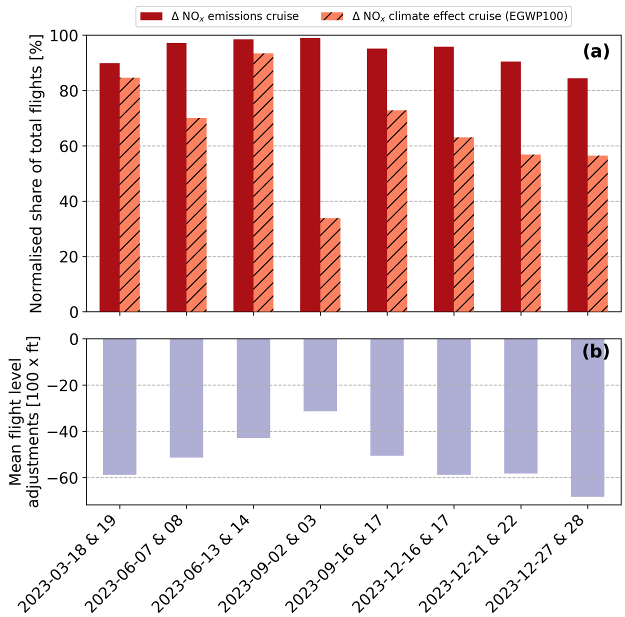

Figure 4. (a) Fraction of flights per day-pair (normalised by the total number of flights) with: higher NO_x emissions (plain bar) and higher climate effect (hatched bar) after contrail-optimisation. (b) Mean flight level adjustments for the temporal vertical detour of contrail-optimisation per day pair.

Denmark, Sweden, Finland, Estonia, and Latvia). We chose these two cases since they both indicate higher NO_x emissions in their contrail-optimised option, but a diverging NO_x climate effect (see Fig. 5). Since the contrail-optimisation in our dataset was performed by flying lower to avoid climate-sensitive areas, and the NO_x climate effect is correlated to the distance to the tropopause, we analyse how the distance between the filed or optimised flight level and the tropopause height changes. The first example shows that on 16 & 17 December, most flight segments would have occurred below the tropopause already. After optimisation, they are pushed down even further. Since the aCCF model primarily shows large gradients along the tropopause (Grewe and Stenke, 2008), the NO_x climate effect function is expected to be similar for both scenarios. However, due to the higher NO_x emissions (and the relation between emissions and climate effect, see Eq. 12), this leads to a large increase in NO_x climate effect of up to +23% ($EGWP_{100}$). In the second example for the day-pair 21 & 22 December it is apparent how the original filed flight segments would have occurred above or at tropopause level. After optimisation, most of these segments are shifted below the tropopause. In this scenario, the NO_x climate effect function changes significantly, compensating for the also higher NO_x emissions. This leads to a much stronger reduction in NO_x climate effect by up to -24% ($EGWP_{100}$). Hence, the two day-pairs are characterised by a different meteorology, with a low and high tropopause. This implies that a downward shift of the optimised trajectories on 21 & 22 December experience a much larger climate impact reduction compared to 16 & 17 December, where both the filed and optimised trajectories are already below the tropopause.

https://doi.org/10.5194/jecats-2026-13
Preprint. Discussion started: 28 July 2026
© Author(s) 2026. CC BY 4.0 License.

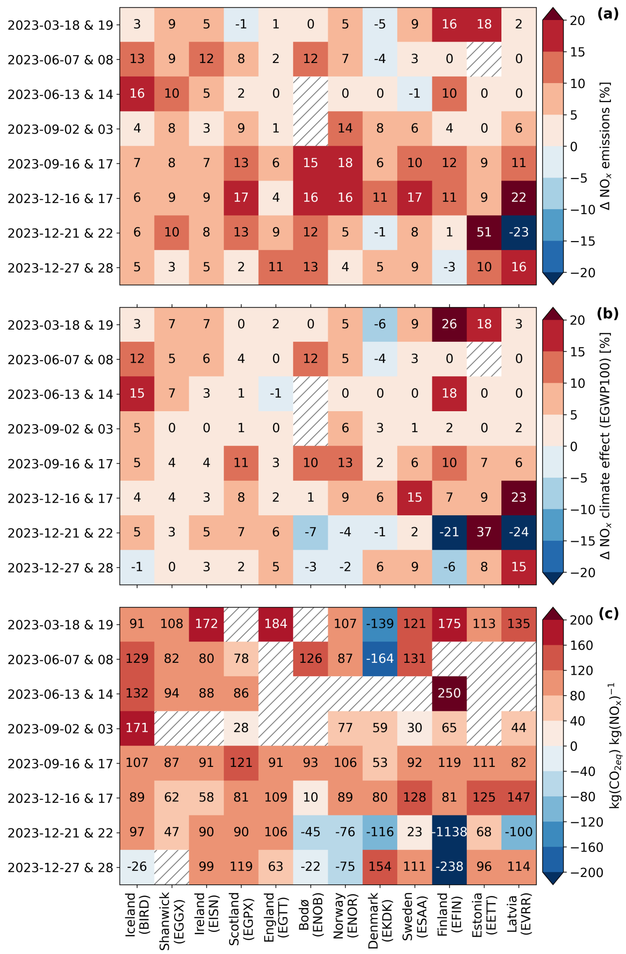

Figure 5. Daily and spatial distribution over the airspaces of: (a) Δ NO_x emissions and (b) Δ NO_x climate effect, where the delta is the difference between filed (baseline) and contrail-optimised trajectories; (c) Normalised change in Δ NO_x climate effect per Δ NO_x emission. Hatched boxes show airspaces with no flights on those days, and also indicate in panel (c) that the calculation could not be performed due to division or multiplication by zero.

To summarise: while NO_x emissions increase over the majority of airspaces and day-pairs, the change in NO_x climate effect is less pronounced. This can be explained by the contrail-optimised flights emitting NO_x at lower (also see Appendix C Fig. C1), less climate-sensitive altitudes, which reduces the NO_x climate effect (Grewe and Stenke, 2008; Köhler et al., 2008; Zengerling et al., 2023). However, flying lower also increases drag, which leads to more thrust, burns more fuel at higher combustion temperatures, and results in both a higher NO_x emission index and higher NO_x emissions. These are obviously opposing effects, which is why the climate effect of NO_x is not linear to its emissions.

https://doi.org/10.5194/jecats-2026-13
Preprint. Discussion started: 28 July 2026
© Author(s) 2026. CC BY 4.0 License.

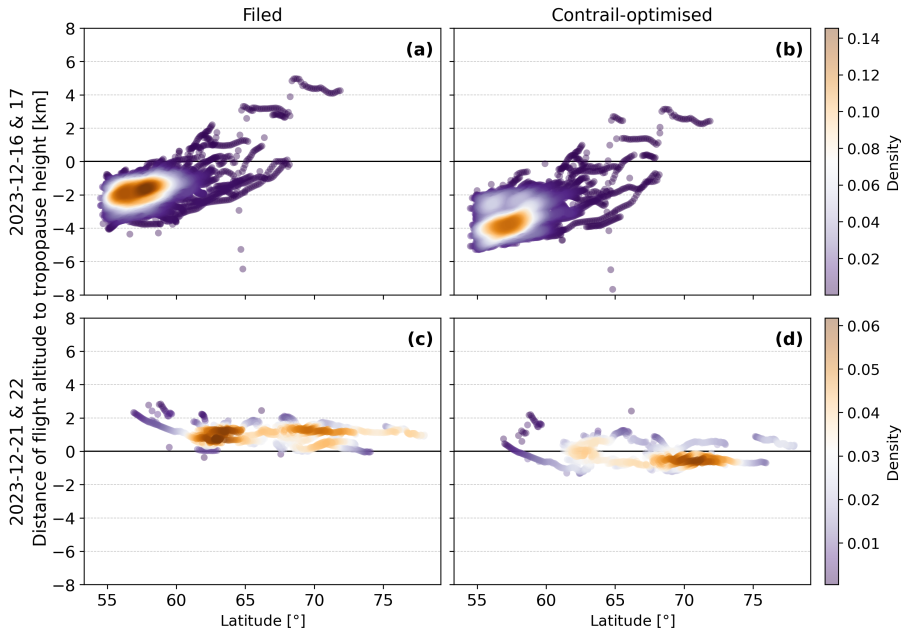

Figure 6. Probability density of flight occurrence in $(\mathrm{km}\times^{\circ})^{-1}$ relative to the distance of filed (a) and contrail-optimised (b) flight altitude to tropopause height and latitude on 16 & 17 December 2023, and filed (c) and contrail-optimised (d) flight altitude to tropopause height and latitude on 21 & 22 December 2023. Only flight segments in airspaces Bodø (ENOB), Norway (ENOR), Denmark (EKDK), Sweden (ESAA), Finland (EFIN), Estonia (EETT), and Latvia (EVRR) are considered that were adapted (vertically) during optimisation and do not fall outside the validity range.

3.3 How much does the overall climate impact mitigation gain change when including NO_x and H_2O?

Within the investigated sample of flights, most contrail-optimised flights achieve a net climate benefit of approximately -16.5% ($EGWP_{100}$) per flight when accounting for both CO_2 and contrail effects (Table 5). Including NO_x and H_2O effects into the evaluation reduces the mean mitigation gain to -11.1% ($EGWP_{100}$). This reduction stands out, given that the mean change in NO_x and H_2O effect (733 $\mathrm{kg(CO_{2eq})}$) is only about 3% of the change in CO_2 and contrail effect ($\sim$26 $\mathrm{t(CO_{2eq})}$). Considering all four species (CO_2, contrails, NO_x, H_2O) further leads to 2% of flights (=88 flights), where the contrail-optimised trajectory shows a larger total climate effect than the filed one ($\Delta\ CO_2 + \Delta\text{Contrail} < 0 \wedge \Delta\text{Total} > 0$). These flights are highlighted with a black cross in Fig. 7. In general, one can observe the large differences in magnitudes among the species: Table 5 shows that the calculated change in contrail climate effect is more than 20 times larger than the change in CO_2. The calculated change in NO_x climate effect is about two thirds of the one in CO_2 and the change in H_2O climate effect is only about 6% of the change in CO_2. Simultaneously, Fig. 7 shows the large differences in magnitudes of absolute delta values for the non-CO_2 species contrails, NO_x, and H_2O. The magnitude of delta contrails is in the range of around -400 to 100 $\mathrm{t}CO_{2eq}$ per flight, compared to only $\pm$ 15 $\mathrm{t}CO_{2eq}$ per flight for the sum of NO_x and H_2O. Hence, the savings due to contrail avoidance outweigh changes

https://doi.org/10.5194/jecats-2026-13
Preprint. Discussion started: 28 July 2026
© Author(s) 2026. CC BY 4.0 License.

Variable	Δ per flight	Δ (%) per flight	Flight segments
Δ Fuel burn	+357 kg	+1.2 %	Entire trajectory
Δ NO_x emission (as NO_2)	+13 kg	+2.5 %	Entire trajectory
Δ CO_2 emission	+1,129 kg	+1.2 %	Entire trajectory
Δ NO_x effect (CO_{2eq}, $EGWP_{100}$)	+733 kg	+1.1 %	Cruise-only
Δ Contrail effect (CO_{2eq}, $EGWP_{100}$)	-26,932 kg	-43.5 %	Entire trajectory
Δ H_2O effect (CO_{2eq}, $EGWP_{100}$)	-64 kg	-1.2 %	Cruise-only
Δ CO_2 + Δ Contrail effect (CO_{2eq}, $EGWP_{100}$)	-25,830 kg	-16.5 %	Entire trajectory
Δ NO_x + Δ H_2O effect (CO_{2eq}, $EGWP_{100}$)	+669 kg	+1.0 %	Cruise-only
Δ Total (CO_{2eq}, $EGWP_{100}$)	-25,161 kg	-11.1 %	Mix
Δ Total (CO_{2eq}, ATR_{100})	-33,095 kg	-12.4 %	Mix
Δ Total (CO_{2eq}, $EGWP_{20}$)	-95,258 kg	-16.2 %	Mix

Table 5. Mean absolute and relative changes per rerouted flight, based on the comparison of filed and contrail-optimised trajectories. Note that fuel burn and NO_x emissions are considered for the whole mission, whereas climate effects are only determined for cruise-phase due to the model limitations (see Sect. 2.2.2).

in the NO_x and H_2O climate effect. However, note that the NO_x and H_2O climate effect is highly sensitive to the aCCF version used, as they reflect different global scalings for different references (see Appendix D for detailed discussion).

We further know from Sect. 2.1 that approximately 15% of flights fail to achieve a net climate benefit when using using reanalysis weather data instead of forecast weather data. This is shown in Fig. 8, where 15% of the bars fall to the right of zero, indicating positive Δ climate effect values. Compared to the 2% of flights for which the change in climate benefit turns positive (i.e. the contrail-optimised trajectory has a larger climate effect than the filed trajectory), this proportion is considerably larger. In Fig. 8 we further illustrate the effect of considering all four species instead of CO_2 and contrails only on the Δ climate effect. It is apparent that the distribution of the change in total climate effect considering all four species (b, in purple) is more tightly concentrated around zero compared to the change in CO_2 and contrails only (a, in orange).

In Fig. 9 we explore the mitigation gain depending on the contribution of the individual climate effects of the filed flights. We map the flights from their ranked contribution on the left to their mitigation gain or loss on the right. Filed flights dominated by contrails (1,599 flights) achieve the largest mitigation gain. However, filed flights dominated by CO_2 and NO_x (1,784 flights) also achieve a large mitigation gain. At the same time, they account for the largest share of flights that failed the optimisation, either due to different weather input or the inclusion of NO_x and H_2O effects during evaluation (shown here as the flow into the $(0-132]$ bin, a bin that accounts for approximately 15% of flights).

https://doi.org/10.5194/jecats-2026-13
Preprint. Discussion started: 28 July 2026
© Author(s) 2026. CC BY 4.0 License.

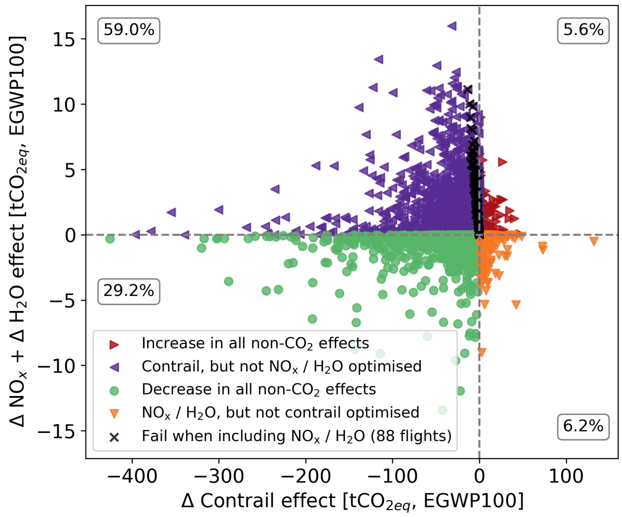

Figure 7. Absolute change in non-CO_2 effects: change in sum of NO_x and H_2O climate effect, plotted against the change in contrail climate effect (tCO_{2eq}, $EGWP_{100}$) per flight after contrail-optimisation. Flights are coloured per quadrant, and the percentage labels represent the share of total flights per quadrant.

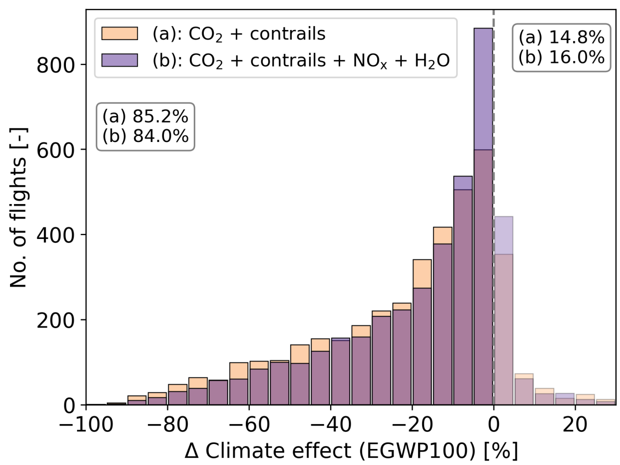

Figure 8. Relative change in aggregated (CO_2 and contrails, and all species) climate effect (tCO_{2eq}, $EGWP_{100}$) per flight after contrail-optimisation. The percentage labels represent the proportion of total flights falling on the left and right sides of zero, respectively.

3.4 What impact does the climate metric choice have on the mitigation gain?

Using ATR_{100} or the $EGWP_{20}$ instead of $EGWP_{100}$ to calculate the climate effect, we observe several changes. The total climate effect reduction rises from -11.1% (-25.2 tCO_{2eq}, $EGWP_{100}$) to -12.4% (-33.1 tCO_{2eq}, ATR_{100}) to -16.2% (-95.3 tCO_{2eq}, $EGWP_{20}$) per flight, on average across all sampled flights (Table 5).

https://doi.org/10.5194/jecats-2026-13
Preprint. Discussion started: 28 July 2026
© Author(s) 2026. CC BY 4.0 License.

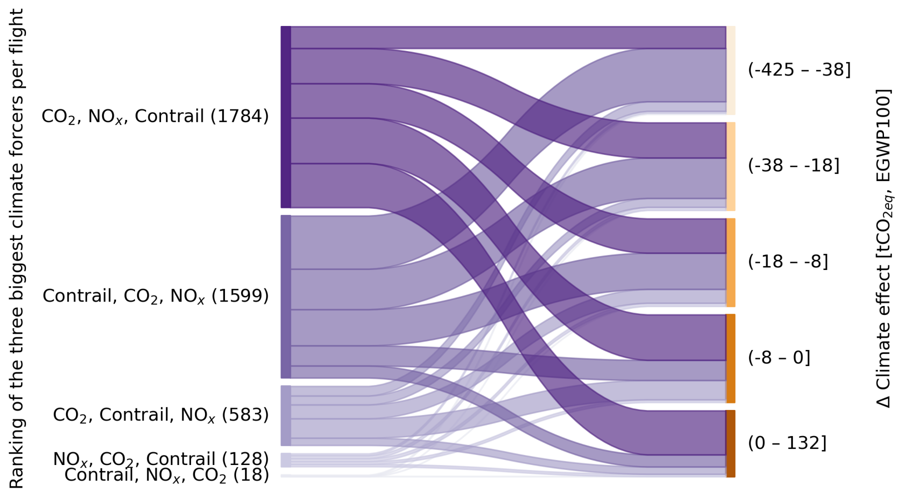

Figure 9. Mapping of ranked contribution of the climate effects of the filed flights (on the left, largest to smallest of the three components CO_2, contrails, and NO_x) to the climate mitigation gain (negative) or loss (positive) on the right in tCO_{2eq}. Numbers in brackets on the left side refer to the number of flights in this group.

Figure 10 compares the contribution of each species to the total climate effect for the filed and contrail-optimised trajectories, as well as for a best estimation reference scenario. When comparing filed with contrail-optimised trajectories, the contribution to the total climate effect is comparable between climate metrics with longer time horizons ($EGWP_{100}$, ATR_{100}) for each species. Changing the metric to a shorter time horizon ($EGWP_{20}$) increases the dominance of short-lived climate forcers (contrails, NO_x) compared to the long-lived species CO_2. One can see that our shares of CO_2 are 4–14 percentage points lower compared to Lee et al. (2021). Our shares of contrails are 8–16 percentage points smaller for filed flights and 17–28 percentage points smaller for contrail-optimised flights. Our NO_x shares are much larger across all metrics and trajectory types. For the reference scenario, we use the global annual CO_{2eq} (GWP_{100} and GWP_{20}) emissions for 2018 by Lee et al. (2021) (their Table 5): CO_2 based on fuel usage of 2018 multiplied with a constant EI_{CO_2}, contrail cirrus with Tg CO_2 basis, net NO_x, and water vapour emissions. We consider the sum of the four as the total, i.e. we do not include aerosols in the calculation. These CO_{2eq} emissions were calculated based on the best estimate ERFs. That means, that fast atmospheric responses are included in the CO_{2eq} estimates using the GWP metric, but no efficacy is considered. The authors claim that the ERF lies within the range of the RF and the RF including efficacies (RF^*), being closer to the latter. Thus, the share of contrails would be slightly smaller if properly accounted for the efficacy. If the contribution of each species to the total climate effect were computed for the 5–95% confidence intervals of the ERF estimates, the resulting shares of the reference scenario would also differ. Further note that the reference scenario covers global annual air traffic, whereas we only consider a sample of ∼4,000 flights with large contrail impact.

https://doi.org/10.5194/jecats-2026-13
Preprint. Discussion started: 28 July 2026
© Author(s) 2026. CC BY 4.0 License.

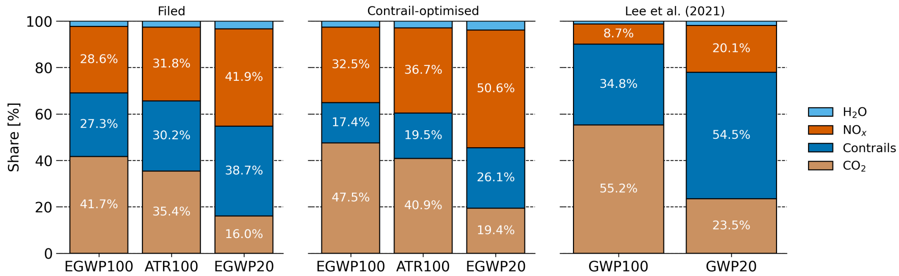

Figure 10. Contribution of each species to the total climate effect (measured in different climate metrics) for the 4,112 filed and contrail-optimised trajectories, and for a best estimation reference scenario. Note that the reference scenario is given in GWP and for a global annual fleet, compared to our results in EGWP (or ATR) and covering a sample of flights traversing the Borealis airspace. See text for details.

As shown in Fig. 11, the largest change in climate effect for all three metrics is observed for contrails, and the smallest for H_2O. For longer time horizons ($EGWP_{100}$, ATR_{100}), the second largest change is attributed to either CO_2 or NO_x. For a shorter time horizon ($EGWP_{20}$) it is NO_x. Only on September 2 & 3, the change in CO_2 is larger than the one from NO_x ($EGWP_{20}$). Hence, changing the metric but keeping the time horizon (i.e., moving from $EGWP_{100}$ to ATR_{100}) only marginally affects the relative ordering of the deltas (first two day-pairs). However, changing the time horizon (i.e., moving from $EGWP_{100}$ to $EGWP_{20}$) reverses the ordering of changes in CO_2 and NO_x for all December day-pairs, and in one case (2 & 3 September) the Δ NO_x changes sign. The change in NO_x, which was net negative for $EGWP_{100}$ and ATR_{100}, is now net positive for $EGWP_{20}$. This does not cause a sign change in the total change though. In addition, the magnitudes of the changes in NO_x and contrail increase. This behaviour is in line with our expectations, emphasising short-lived climate forcers. Comparing our results with those from Kirschler et al. (2026) (their Fig. 5), both works agree that all climate metrics indicate successful climate mitigation.

4 Discussion and limitations

In general, our results are largely consistent with previous trajectory optimisation studies: with little extra fuel, an overall climate benefit can be achieved (Table 6). This holds true for different climate metrics and considering four species (CO_2, contrails, NO_x, H_2O). According to literature, contrail mitigation seems to be relatively consistently at 20–40% for different models, and fuel penalties per flight are mostly at 0–1%, with fleet-wide values lowered to 0.11–0.37%. There are a few discrepancies though when comparing our results with other modelling studies: First, it should be noted that some studies report fleet-wide fuel increases rather than per-flight values (e.g. Martin Frias et al. (2024); Piontek et al. (2026)). Whenever possible, these were converted. Second, care must be taken to ensure that all relevant species are accounted for when assessing the total climate benefit. For instance, our study reports a $\Delta EF_{contrail}$ of -43.5%, but the overall net climate benefit is only -11 to -16% ($EGWP_{100}$, ATR_{100}, $EGWP_{20}$). Teoh et al. (2020) report a $\Delta EF_{contrail}$ of -59%, and a $\Delta EF_{contrail,CO_2}$ over 100 years of -35.6%. Martin Frias et al. (2024) report a $\Delta EF_{contrail}$ of -73%, and their total net climate benefit (contrail, CO_2) is -22% (GWP_{20}), which is consistent with our results. In addition, the shorter the time horizon (e.g. 20 years), the larger the claimed

https://doi.org/10.5194/jecats-2026-13
Preprint. Discussion started: 28 July 2026
© Author(s) 2026. CC BY 4.0 License.

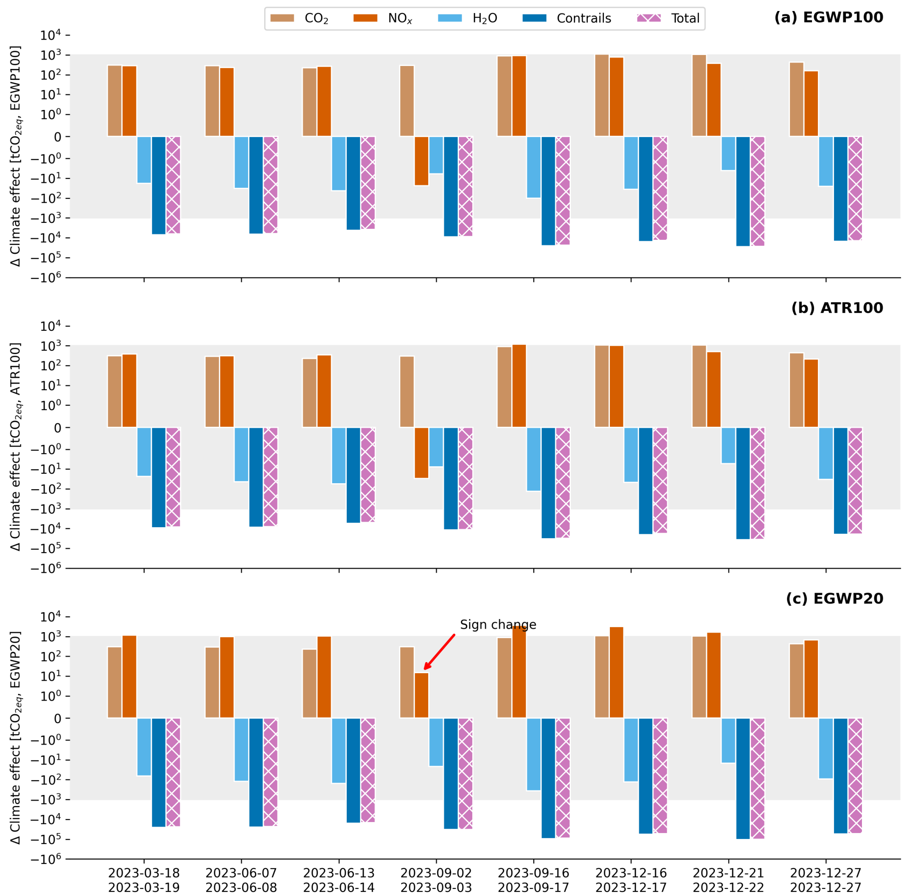

Figure 11. Change in climate effect per climate forcer and day-pair when comparing filed with contrail-optimised flights for a) $EGWP_{100}$, b) ATR_{100}, and c) $EGWP_{20}$. Note that the y-axis is on a logarithmic scale. The grey shading facilitates to recognize the magnitude differences across species.

climate benefit. This is seen in our results (the benefit increases from -11% to -16%), but also in the largest climate benefit of all considered studies (-50%) claimed by Lührs et al. (2021). Furthermore, those studies optimise and evaluate for the same climate metric, whereas in our work the metric is additionally changed during evaluation to test for robustness. Another point to consider is the inclusion of the efficacies. For instance, Piontek et al. (2026) use the GWP_{100} without efficacies and claim a net climate benefit of -18%. They further mention in their limitations that using a contrail efficacy, such as the one by Bickel et al. (2025) used in our work, would reduce the contrail climate benefit substantially. Third, some studies take a more theoretical approach, optimising trajectories without accounting for airspace structure or operational flight procedures (e.g. Grewe et al. (2017); Castino et al. (2024)), whereas other studies consider operational constraints during optimisation (e.g. Martin Frias et al. (2024), and our work). Lastly, the regions considered vary from study to study, leading to different weather conditions and air traffic densities. These regional differences impact the patterns of contrail formation and the NO_x climate effect, which

https://doi.org/10.5194/jecats-2026-13
Preprint. Discussion started: 28 July 2026
© Author(s) 2026. CC BY 4.0 License.

might change the magnitude of claimed net climate benefit when the same methodology would be applied to other regions. Yet, despite those differences, modelling studies consistently point in the same direction: contrail avoidance is an effective mitigation option.

While our results are derived for the Borealis region, the underlying methodology is general and can in principle be applied to other regions, seasons, and traffic scenarios. However, seasonal and regional limitations of the aCCFs and sensitivity to weather input of CoCiP should be taken into account (see Sect. 4.1), and airspaces must permit free-routing. In terms of ATC constraints from flight level adjustments, Piontek et al. (2026) found a small increase in congestion and a significant increase in separation conflicts of flights using their polygon-based optimisation approach for vertical trajectory adjustments. We did not investigate the impact on operations of our contrail-optimised flights, but given the cost-based optimiser used in our work with finer possible adjustments, we would expect less disturbances. Furthermore, it should be notes that since only flights with large contrail impact were evaluated, the -11% to -16% in climate benefit is not directly transferable to a global fleet. That said, whether the magnitude of the reported effects transfers directly to other regions, seasons, or traffic scenarios remains to be validated.

Despite successful climate mitigation throughout all three considered climate metrics, we saw that the mean net climate benefit per flight ranges from -25.2 tCO_{2eq} ($EGWP_{100}$) to -95.3 tCO_{2eq} ($EGWP_{20}$). While this may be acceptable from a purely climate perspective, it has significant economic implications: should non-CO_2 effects be assigned a price, a factor of four difference would substantially change the economics of contrail-optimal flight planning.

The results are further subject to uncertainties in the calculation of the individual climate effects. Here, we recap our three major research questions (RQs) and how uncertainties might impact our answers:

- **RQ1**: In our study we find that contrail-optimised routings lead to lower flight altitudes. Flying lower mostly increases the NO_x emissions (Fig. 3), but simultaneously reduces the NO_x climate effect per emitted NO_x (Köhler et al., 2008; Frömming et al., 2012; Søvde et al., 2014; Matthes et al., 2021; Dahlmann et al., 2016). These opposing effects differ considerably in their uncertainty: the emissions are associated with a small uncertainty range (around 10% (DuBois and Paynter, 2006; Harlass et al., 2024)), while the climate effect carries a much wider range (Lee et al., 2021). The net NO_x climate effect reported by Lee et al. (2021) for example gives estimates for the NO_x-RF ranging from net cooling to net warming, and estimates for the NO_x-ERF ranging from near zero to net warming. While the absolute value of the NO_x-RF has large uncertainties, the effect of flying lower was assessed consistently in a model intercomparison (Søvde et al., 2014; Matthes et al., 2021). Including these uncertainties into the modelling would affect the simulation results for the climate effect per emission, whereas the modelling of the emissions themselves are not expected to change much. Since the NO_x climate effect is the product of the two, the results may change, though the direction and magnitude of this change still has to be determined. Another point to consider is that we evaluated flights with large contrail impact only. For flights that do not form persistent warming contrails, the NO_x effect might play a bigger role.

- **RQ2**: Non-CO_2 effects are all subject to considerable uncertainty: this applies not only to NO_x, as noted above, but also to contrails and H_2O (Lee et al., 2021). So what would happen to the total mitigation gain in case we were overestimating

https://doi.org/10.5194/jecats-2026-13
Preprint. Discussion started: 28 July 2026
© Author(s) 2026. CC BY 4.0 License.

Study	No. flights	Rerouted flights	Days	Region	Model	CO_2	Contrails	NO_x	H_2O	Δ Fuel	Δ Climate	Climate metric
Grewe et al. (2017)	800	all	8	North-Atlantic	CCF	✓	✓	✓	✓	+1.0%*	-10%	ATR_{20} [K]
Yin et al. (2018a)	103 per day	all	365	North-Atlantic	EMAC†		✓			+0.2%	-42%	$km_{contrail}$
Rosenow et al. (2019)	13,584	all	1	Europe	ISSR penalty‡		✓			+0.05%	-32%	GWP
Teoh et al. (2020)	149,000	1.7%	42	Japan	CoCiP	✓	✓			+0.27%	-35.6%	EF_{100} [J]
Matthes et al. (2020)	2,000	all	1	Europe	aCCF	✓	✓	✓	✓	+0.50%	-46%	ATR_{20} [K]
Lührs et al. (2021)	13,000	all	1	Europe	aCCF	✓	✓	✓	✓	+0.75%	-50%	ATR_{20} [K]
Castino et al. (2024)	100 per day	all	31	North-Atlantic	aCCF	✓	✓	✓	✓	+1.86%	-7.9%	ATR_{20} [K]
Martin Frias et al. (2024)	84,839	12.9%	28	United States	CoCiP	✓	✓			+0.11%**	-22%	GWP_{20}
Piontek et al. (2026)	145,092	9.0%	16	Northern Europe	CoCiP, aCCF	✓	✓	✓	✓	+0.37%**	-18%	GWP_{100}
This work	∼150,000	4,112	16	Northern Europe	CoCiP, aCCF	✓	✓	✓	✓	+1.2%	-11% / -16%	Multiple

Table 6. Selection of climate trajectory optimisation studies covering >500 flights. Species marked with a checkmark are included in the 'Δ Climate' estimate. Note that some studies report a Pareto front of climate-cost optimal solutions (e.g. Grewe et al. (2017); Yin et al. (2018a); Castino et al. (2024)), from which we selected one that also satisfies our study's constraint of limiting extra fuel to a maximum of 2%. †Routing decision is based on EMAC's submodel CONTRAIL (which estimates the potential contrail coverag, see esupplement of Grewe et al. (2014b)), and the evaluation of changes is performed with EMAC (Jöckel et al., 2010). ‡Flying through an ice-supersaturated region (ISSR) is assigned a cost of 32 $tCO_{2eq}\ h^{-1}$. *Considering cost, not fuel. **Considering the fleet-wide fuel increase.

https://doi.org/10.5194/jecats-2026-13
Preprint. Discussion started: 28 July 2026
© Author(s) 2026. CC BY 4.0 License.

contrails and underestimating NO_x and H_2O? First of all, there is quite a margin in between the mean contrail reduction per flight (-26 $\mathrm{tCO_{2eq}}$) and the NO_x (+0.73 $\mathrm{tCO_{2eq}}$) and H_2O (+0.064 $\mathrm{tCO_{2eq}}$) effects, $EGWP_{100}$. If we took the lower bound of the ERF estimates by Lee et al. (2021) for contrails (-70%) and the upper bounds of the NO_x (+66%) and H_2O effects (+60%) to approximate over- and underestimations of the non-CO_2 effect, we would get -8.08 $\mathrm{tCO_{2eq}}$ (contrails), +1.22 $\mathrm{tCO_{2eq}}$ (NO_x), and +0.1 $\mathrm{tCO_{2eq}}$ (H_2O) per flight. Thus, the mean benefit through contrail avoidance would still exceed the penalties. Applying these changes on each individual flight would result in 9.5% of flights turning net warming after contrail-optimisation (compared to 2% before) (Appendix E Fig. E1).

– **RQ3**: We derive our CO_{2eq} estimates relative to the CO_2 climate effect by Gaillot et al. (2023) (Eq. 3). Latest estimates of the specific AGWP of CO_2 by Dahlmann et al. (2025) (their Table 6) are 15.5% lower for a time horizon of 100 years, and 1.1% higher for a time horizon of 20 years, mainly due to different background concentrations of CO_2. That means that absolute CO_{2eq} estimates for longer time horizons would be larger, whereas the estimates would barely change for shorter time horizons.

In addition, optimizing using forecast weather leads to ∼11% of flights failing contrail avoidance, and ∼15% failing overall climate mitigation when CO_2 is included (Sect. 2.1). Although forecast accuracy may improve over time and reduce this error, natural weather variability (Wilhelm et al., 2021) will always remain, meaning weather-related uncertainty will continue to play a role.

4.1 Limitations

Limitations of our study range from the flight trajectory optimisation, to air space restrictions, and to the modelling approaches in the climate impact evaluation. A limitation of the flight trajectory optimisation algorithm is the constraint of allowing at most one deviation from the filed trajectory, meaning the full optimisation potential is not exploited. Additionally, real-world ATC constraints are not accounted for: in practice, after a flight level change to a lower altitude, an aircraft may be unable to return to its optimal cruise altitude immediately when the optimiser suggests it, as it must re-enter the queue. This would result in a larger fuel and CO_2 penalty due to extended flight at suboptimal altitudes.

We discovered three model limitations in the aCCFs we use in our methodology, causing large deviations in the estimated NO_x and H_2O climate effect. First, the variability of different versions of the aCCF model (Appendix D Fig. D1). The question of which version best reflects the actual climate effect remains an active area of research. The MRV (Eichinger et al., 2025) suggests the usage of version 1.0A (Matthes et al., 2023), and efforts are underway to develop dedicated models for specific regions, meteorological conditions, and seasonal variations, which is promising. To account for uncertainties, Rao et al. (2024) further implemented the first version of probabilistic aCCFs (paCCFs) for ozone. Once such a model is available for other species (methane, water vapour), paCCFs could be a great addition to aCCFs. Second, following a vertical optimisation approach, flight trajectories are usually pushed to lower altitudes (Lührs et al., 2021; Zengerling et al., 2023). The aCCF model has limited altitudinal coverage that does not fully capture cruise altitudes, leading to flight segments being pushed outside its valid band (Appendix C Fig. C1). These flight segments can thus not be considered in the analysis (Appendix C Fig. C2), mak-

https://doi.org/10.5194/jecats-2026-13
Preprint. Discussion started: 28 July 2026
© Author(s) 2026. CC BY 4.0 License.

ing it hard to provide a complete picture of the actual change in climate effect. (How the NO_x climate effect would change if a different validity range were chosen is shown in Appendix C Fig. C3). Third, the horizontal coverage of the aCCFs. Van Manen and Grewe (2019) claim that the aCCFs can be applied to the northern hemisphere for 30–60° N. Maruhashi et al. (2022) further show that transport and NO_x-ozone impact patterns over North America and Eurasia behave similarly to one another, but distinctly from other regions. However, the investigated regions only partially overlap with the Borealis airspaces (45–82° N) in the present study. We therefore suggest future work to investigate the aCCF validity beyond the current vertical and lateral boundaries.

Other limitations come from the CoCiP model that we use to estimate the contrail climate effect. Akhtar Martínez et al. (2025) found that CoCiP may underestimate the impact of long-lived contrails, since it does not fully capture later phases of the contrail evolution. In our data, only 2.5% of all flight segments cause contrails that survive at least 7 hours. Therefore, we do not expect large changes in our results. The authors also found that CoCiP is sensitive to relative humidity and wind shear. However, they acknowledge that their input weather data is synthetic and recommend further comparisons using more realistic meteorology. Another limitation of this study is that we do not include volatile particulate matter (vPM) emissions for the prediction of contrails. They are estimated to play a major role in the formation of contrails for the low-soot regime (Voigt et al., 2025). In our data, the 0.5th–99.5th percentile range of the nvPM EI number spans from 2.0^{14} kg^{-1} to 8.6^{15} kg^{-1} for both filed and contrail-optimised trajectories. This indicates that 99% of values fall within the soot-rich regime (Yu et al., 2024), so no major changes would be expected for our results including vPM emissions.

5 Conclusions

The aim of this study is to assess the robustness of the climate benefit of contrail-optimised trajectories for the Borealis airspace. Specifically, it investigates whether trajectories optimised to avoid contrails under operational constraints (forecast meteorological data, prescribed fuel and time penalties) and a given climate metric continue to yield a net climate benefit when evaluated against reanalysis data, extended to include NO_x and H_2O effects, and assessed across alternative climate metrics. Our model setup follows the recommendations of the MRV and uses the models CoCiP (contrails) and aCCFs (NO_x, H_2O) to evaluate the non-CO_2 climate effect of approximately 4,000 real-world flights with large contrail impact traversing Northern Europe in 2023. Fuel consumption, emissions, and climate effect estimates were then compared to literature.

We found that the ratio of climate benefit to additional fuel use (+1.2% fuel ⇒ -43.5% contrails and -11% to -16% climate impact) falls within the range reported in the literature (see Table 6). The main findings can be summarised as follows:

– **RQ1**: On average across the ∼4,000 flights with large contrail impact, contrail-optimised flights emit 2.5% more NO_x compared to the baseline, whereas the NO_x climate effect only increases by 1.1% ($EGWP_{100}$). In other words, 93% of flights emit more NO_x, but only 65% of all flights also show an increased NO_x climate effect due to the lower flight altitude, where the climate effect per unit mass of NO_x emitted is reduced. Given the large uncertainty in modelling the transport pathways of emitted NO_x, however, one should be careful about extrapolating the results.

https://doi.org/10.5194/jecats-2026-13
Preprint. Discussion started: 28 July 2026
© Author(s) 2026. CC BY 4.0 License.

- **RQ2**: Including NO_x and H_2O effects in the estimate of the net climate benefit of our contrail-optimised flights reduces the mitigation benefit from -16.5% (considering contrails and CO_2 only) to -11.1% (considering all four species), $EGWP_{100}$. Despite the change in mitigation benefit, the majority of flights (98%) still achieve a net gain, because contrail effects are much larger in magnitude than NO_x and H_2O effects for our flights with large contrail impact. Even when accounting for potential over- and underestimations of these non-CO_2 effects, more than 90% of flights still achieve a gain. The more critical factor is the meteorology: Using forecast weather instead of reanalysis weather results in 15% of flights where contrail-optimisation fails to achieve a net climate benefit. This impact exceeds that of including additional non-CO_2 species, at least for our flights with large contrail impact.

- **RQ3**: The climate metric affects the magnitude of the total mitigation gain, but does not result in a net sign change of it. The climate benefits under the $EGWP_{100}$ and ATR_{100} metrics are comparable (-11.1% and -12.4%, respectively), indicating the robustness of our contrail-optimised flights over different metrics that express a similar objective. Using the $EGWP_{20}$ metric during evaluation, and hence, changing the focus to avoiding additional warming in the next two decades, even increases the mitigation gain (-16.2%).

We conclude that optimising for contrails alone is feasible to mitigate the climate impact for flights with large contrail impact and considering vertical trajectory adjustments, at least as long as the contrail climate effect is substantially larger than the other non-CO_2 effects. For flights without significant contrail impact, NO_x and H_2O effects should be included in trajectory-optimisation strategies, since their effects might play a bigger role compared to CO_2 than for large contrail impact flights. When doing so, it is important to ensure a consistent model setup with consistent climate metric conversions to make results comparable across studies.

Appendix A: Project overview

This study is related to the work by Piontek et al. (2026) through shared project funding under the SESAR (Single European Sky ATM Research) project CONCERTO (Dynamic Collaboration to Generalize Eco-friendly Trajectories). Both remain standalone studies though. While Piontek et al. (2026) address exercise 1, the present work stems from exercise 2.1. A comparison of the two exercises is provided in Table A1.

Piontek et al. (2026) (Sect. 2.4) proposed a sample selection of 16 days in 2023 for the Borealis airspace: selecting one weekday and one weekend day per season, each further split into one normal and one high-impact day, when considering the total climate effect. Both studies assess the mitigation potential of trajectory optimisation for this period. The air traffic data used in both studies is based on filed flight plans submitted to the network manager, that were converted into trajectories with a one-minute resolution. The two studies further share a pre-tactical and vertical-deviation-only approach, and follow a similar model setup.

However, the study by Piontek et al. (2026) first calculates climate-sensitive areas and their probability based on the ECMWF ERA5 10-member ensemble, and applying the CoCiP and aCCF models for contrails and NO_x and H_2O, respectively. These

https://doi.org/10.5194/jecats-2026-13
Preprint. Discussion started: 28 July 2026
© Author(s) 2026. CC BY 4.0 License.

	CONCERTO Exercise 1 **Piontek et al. (2026)**	**CONCERTO Exercise 2.1** **This work**
Day selection	16 days in 2023	16 days in 2023
Study region	Borealis	Borealis
No. flights	∼145,000	∼150,000
Rerouted flights	9%	4,112
Planning horizon	pre-tactical	pre-tactical
Optimisation approach	avoid climate-sensitive regions (polygon-based)	minimise climate-impact costs (cost-based)
Trajectory adjustments	vertical only	vertical only
ATM constraints	–	trajectory adjustments only at ATM fixes change in flight sector occupancy is considered
Meteorology	ERA5 reanalysis ensemble	HRES forecast (optimisation) ERA5 reanalysis (evaluation)
Climate models	CoCiP, aCCF	CoCiP, aCCF
Species	CO_2, Contrails, NO_x, H_2O	CO_2, Contrails (optimisation) CO_2, Contrails, NO_x, H_2O (evaluation)
Climate metric	GWP_{100}	$EGWP_{100}$ (optimisation) $EGWP_{100}$, ATR_{100}, $EGWP_{20}$ (evaluation)
Contrail efficacy	1.0	0.42 (optimisation), 0.21 (evaluation)

Table A1. Comparison of the two CONCERTO exercises and their model setups.

areas are technically polygons on each flight level for different confidence intervals. The authors then optimise trajectories by avoiding these areas considering different constraints.

585 We optimise trajectories using a cost function that quantifies the climate impact of contrail formation, modelled via CoCiP using ECMWF HRES forecast data as meteorological input. The optimiser estimates the warming contrails of all flights and proposes alternatives to the ones with the largest warming, considering constraints of less than 2% extra fuel, less than 5 minutes extra flight time and more than 5 $\mathrm{t(CO_{2eq})}$ of climate benefit, $EGWP_{100}$. We then calculate the occupancy percentiles for each flight sector before and after optimisation, and select the proposed alternatives that show the least effect in flight sector 590 workload. We then evaluate the climate benefits using deterministic ERA5 reanalysis data, and applying the same models (CoCiP, aCCFS) as Piontek et al. (2026). We further evaluate our results using three different climate metrics.

https://doi.org/10.5194/jecats-2026-13
Preprint. Discussion started: 28 July 2026
© Author(s) 2026. CC BY 4.0 License.

Appendix B: Model setup to generate contrail-optimised trajectories

Aircraft performance was modelled using BADA3 (EUROCONTROL, 2022), accessed via the pycontrails-bada library (v0.6.2) (Shapiro et al., 2025), with engines selected from the BADA database based on aircraft type. We simulated contrail evolution using CoCiP Grid (pycontrails v0.54.5) (Engberg et al., 2025; Shapiro et al., 2025), applying humidity scaling via an exponential boost correction (ExponentialBoostHumidityScaling: rhi-adj=0.9779, rhi-boost-exponent=1.635, clip-upper=1.65). We did not account for contrail-contrail overlap. The integration used a 5-minute time step, and we tracked contrails for a maximum age of 14 hours. We recomputed aircraft heading from the mean track between waypoints with wind correction applied. Trajectory optimisation relied on ECMWF HRES forecast data (ECMWF, 2024), with each flight optimised using a forecast initialised between 9 and 21 hours before take-off. Each optimisation run produced zero or one optimised trajectory per flight, and multiple runs could be performed with varying tuning parameters. Cloud ice water content was handled using the default pycontrails treatment. The optimisation was deterministic, with no ensemble treatment applied. Regarding the climate metric, CO_2 emissions were derived from fuel burn using an emission index of $\mathrm{EI}_{\mathrm{CO_2}} = 3.16\ \mathrm{kg\ kg^{-1}}$ (ICAO, 2018). The contrail climate impact was computed as energy forcing (EF) using pycontrails and subsequently converted to EGWP_{100}, assuming an efficacy of 0.42. Climate effects from other species were not computed using forecast data.

Appendix C: Vertical coverage and model sensitivity

The aCCF model was derived from the CCFs, which quantify the climate response for standardised emissions between 200 hPa and 400 hPa. However, as pointed out in Sect. 2.2.2, many (cruise) flight segments fall outside this range (Fig. C2). We further

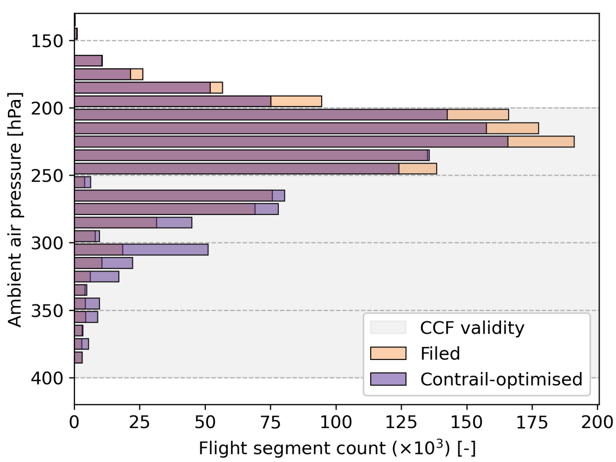

Figure C1. Distribution of waypoints along altitudes. About a quarter of flight segments occurs above the CCF validity coverage. It is also visible that optimised trajectories are clearly pushed to lower altitudes.

decided to only evaluate flight segments where both the filed and contrail-optimised segments are within the validity range

https://doi.org/10.5194/jecats-2026-13
Preprint. Discussion started: 28 July 2026
© Author(s) 2026. CC BY 4.0 License.

(Sect. 2.2.2). This is illustrated in Fig. C2. Lastly, Fig. C3 shows the sensitivity of choosing a validity range on the NO_x

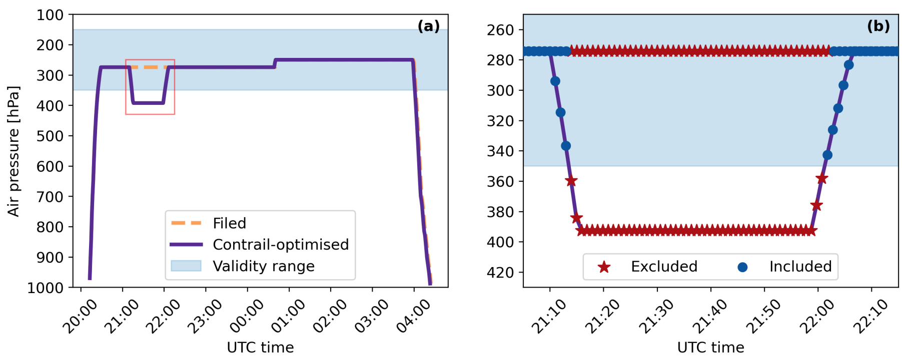

Figure C2. Example trajectory for (a) full flight and (b) part of the flight to show which waypoints are considered in the evaluation. Since the contrail-optimised trajectory leaves the valid zone and no climate effect can be determined for these waypoints, the original waypoints have to be excluded as well in the calculation of the delta. This situation occurs in 13.7 % of all flights. The chosen validity range is described in Sect. 2.2.2.

climate effect.

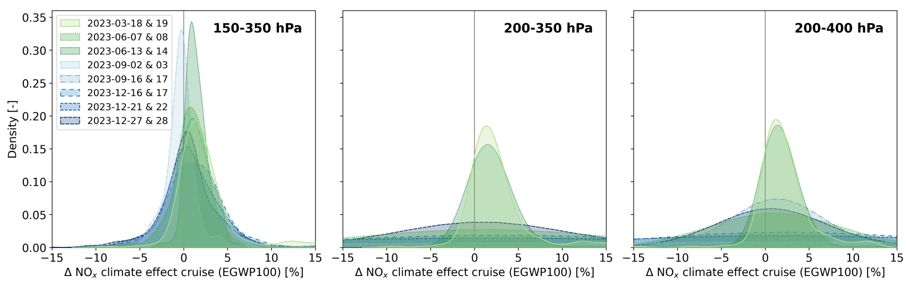

Figure C3. Distribution of relative change in NO_x climate effect in $EGWP_{100}$ per flight after contrail-optimisation for three different cruise pressure level ranges. The baseline is the middle plot (200–350 hPa), where all model features are fully captured, i.e. the aCCFs produce results correlated to the CCFs. However, as seen in Fig. C1, that causes about a quarter of flight segments to be excluded, significantly altering the distribution as seen in the left plot (150–350 hPa). Extending the range in the opposite direction, i.e. into regions where the aCCFs diverge from the CCF, has a negligible effect on the aggregated results as seen in the right plot (200–400 hPa). Yet, we found that for certain airspaces and on specific days, this extension of validity range does impact the results.

https://doi.org/10.5194/jecats-2026-13
Preprint. Discussion started: 28 July 2026
© Author(s) 2026. CC BY 4.0 License.

Appendix D: aCCF versions

Table D1 shows the aCCF scaling factors by which all coefficients of the baseline formulas from Van Manen and Grewe (2019) (for species H_2O, O_3, CH_4) and Yin et al. (2023); Dietmüller et al. (2023) (for species contrails and CO_2) are divided to obtain the scaled versions. All three aCCF versions are given in a pulse emission scenario with a 20 year time horizon (P-ATR_{20}). This is because aCCFs are derived from CCFs, and CCFs follow the pulse emission scenario integrated over 20 years from Aamaas et al. (2013) (see Frömming et al. (2021), their Sect. 2.4). Hence the emissions differ in the used metric and in a scaling of annual mean values to a specific reference. Note that spatial sensitivity is unchanged.

aCCF version	H_2O	O_3	CH_4	Contrail	CO_2
Van Manen and Grewe (2019)	1	1	1	-	-
Yin et al. (2023) and Dietmüller et al. (2023)	1.92	1.97	2.03	1.00	1.00
Matthes et al. (2023)	3.00	11.00	35.00	3.00	1.00

Table D1. Scaling factors by which all coefficients of the baseline aCCFs from Van Manen and Grewe (2019) are divided to obtain the scaled versions. The baseline for the contrail aCCF and CO_2 aCCF is Yin et al. (2023); Dietmüller et al. (2023). The climate metric is P-ATR_{20} for all three aCCF versions.

β	H_2O	O_3	CH_4	Contrail
SS2000 → BR2008	0.520	0.508	0.492	0.509

Table D2. Backward calculation factors to get from the climate response function of Sausen and Schumann (2000) (SS2000) to Boucher and Reddy (2008) (BR2008), to be compatible with the conversion factors in Dahlmann et al. (2025).

Figure D1 illustrates the sensitivity of the results to the choice of model, with each model yielding different results. While the spatial dependencies and sensitivities between the three aCCF versions are the same, the absolute values differ due to different assumptions. While Van Manen and Grewe (2019) used the temperature regression formula from Boucher and Reddy (2008), Yin et al. (2023), Dietmüller et al. (2023) and Matthes et al. (2023) used the regression formula from Sausen and Schumann (2000). For P-ATR_{20}, this yields in a difference of a factor of around two. Note that this factor changes for different climate metrics and time horizons: While using Boucher and Reddy (2008) for ATR_{20} almost doubles the absolute values, for ATR_{100} the increase is less than 15%. The aCCFs by Matthes et al. (2023) are based on Yin et al. (2023), but include alignments from aCCFs to the climate response model AirClim (Grewe and Stenke, 2008; Dahlmann et al., 2016), to receive comparable absolute values as in AirClim. The CO_2 estimates by the aCCFs are all based on the AirClim version using Sausen and Schumann (2000) and therewith only about half of what the best estimate by Gaillot et al. (2023) suggests, which uses Boucher and Reddy (2008). Using the AirClim version with temperature regression from Boucher and Reddy (2008) as in Dahlmann et al. (2025), would result in similar CO_2 estimates as Gaillot et al. (2023) report.

https://doi.org/10.5194/jecats-2026-13
Preprint. Discussion started: 28 July 2026
© Author(s) 2026. CC BY 4.0 License.

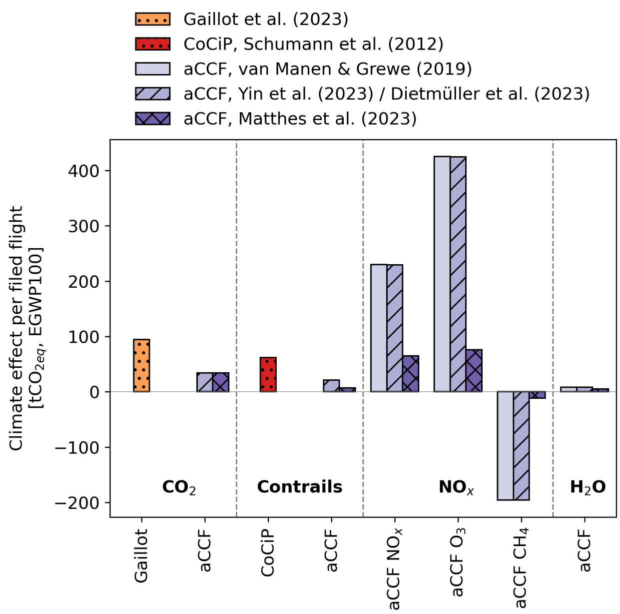

Figure D1. Mean climate effect per filed flight (considering the full traffic set of 4,112 flights) in tCO_{2eq} ($EGWP_{100}$) for different species and the three aCCF versions (Van Manen and Grewe, 2019; Yin et al., 2023; Dietmüller et al., 2023; Matthes et al., 2023). CO_2 values are estimated with Eq. (3), whereas NO_x, O_3, CH_4, and H_2O are calculated with their respective aCCF (see Table D1 for the precise scaling factors). To convert the results from CO_2 and non-CO_2 to the same unit, we follow the procedure explained in Sect. 2.3 which uses the conversion factors between individual climate metrics by Dahlmann et al. (2025) and additionally use the backward calculation factors from Table D2 for the Yin et al. (2023); Dietmüller et al. (2023); Matthes et al. (2023) aCCF versions.

https://doi.org/10.5194/jecats-2026-13
Preprint. Discussion started: 28 July 2026
© Author(s) 2026. CC BY 4.0 License.

Appendix E: Impact of uncertainties on simulation outcome

In case our model setup overestimates contrail formation and underestimates NO_x and H_2O effects, the net mitigation gain of trajectory optimisation would be affected. Such a change is illustrated in Fig. E1, where the number of flights achieving a net climate benefit is reduced by 5.4 to 10.9 percentage points, depending on the considered species.

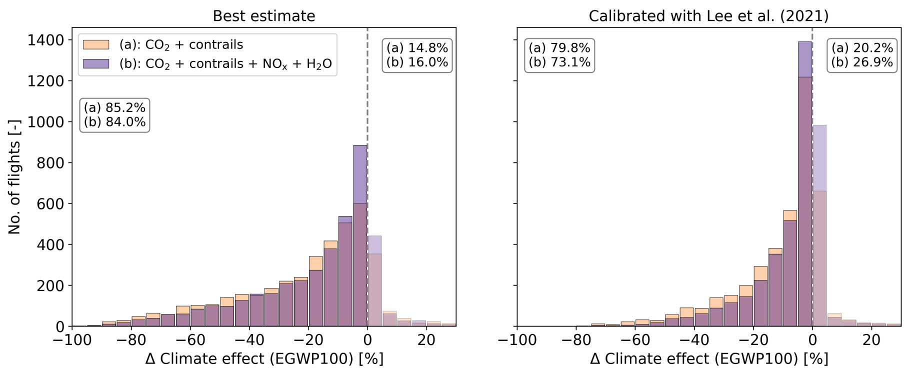

Figure E1. Relative change in aggregated (CO_2 and contrails, and all species) climate effect (tCO_{2eq}, $EGWP_{100}$) per flight after contrail-optimisation; for the simulation results (best estimate), and for approximated over- and underestimated simulation results based on ERF confidence intervals from Lee et al. (2021). The percentage labels represent the proportion of total flights falling on the left and right sides of zero, respectively.

Code and data availability. The dataset used for the analysis is available at https://doi.org/10.4121/16ec2954-a493-41c8-b3f9-f17e9331c46b. The code of the processing pipeline and the notebooks to reproduce the results of this paper are available at https://doi.org/10.4121/cbdafa47-709d-45da-86e1-7fed28ec3582.

Author contributions. JS, FY, and VG developed the concepts presented in this paper. JC and SNA optimised the trajectories and prepared the dataset. JS performed the post-processing and analysed the results presented in this study. JS, FY, FC, and VG discussed the results. KD, DP and JS set up the climate metric conversion. All co-authors contributed to the discussion and the revision of the paper.

Competing interests. Some authors are members of the editorial board of the Journal of Environmentally Compatible Air Transport System (JECATS).

https://doi.org/10.5194/jecats-2026-13
Preprint. Discussion started: 28 July 2026
© Author(s) 2026. CC BY 4.0 License.

Acknowledgements. This study has received funding from the SESAR 3 Joint Undertaking CONCERTO under grant agreement No. 101114785, which is part of the Aviation Green Deal flagship within the European Green Deal. Claude (Anthropic) was used to assist with data analysis and manuscript editing. All outputs were reviewed and validated by the authors.

https://doi.org/10.5194/jecats-2026-13
Preprint. Discussion started: 28 July 2026
© Author(s) 2026. CC BY 4.0 License.

References

Aamaas, B., Peters, G. P., and Fuglestvedt, J. S.: Simple emission metrics for climate impacts, Earth System Dynamics, 4, 145–170, https://doi.org/10.5194/esd-4-145-2013, 2013.

Akhtar Martínez, C., Eastham, S. D., and Jarrett, J. P.: Zero-dimensional contrail models could underpredict lifetime optical depth, Atmospheric Chemistry and Physics, 25, 12 875–12 891, https://doi.org/10.5194/acp-25-12875-2025, 2025.

Baneshi, F., Soler, M., and Simorgh, A.: Conflict assessment and resolution of climate-optimal aircraft trajectories at network scale, Transportation Research Part D: Transport and Environment, 115, 103 592, https://doi.org/10.1016/j.trd.2022.103592, 2023.

Bickel, M., Ponater, M., Burkhardt, U., Righi, M., Hendricks, J., and Jöckel, P.: Contrail Cirrus Climate Impact: From Radiative Forcing to Surface Temperature Change, Journal of Climate, 38, 1895–1912, https://doi.org/10.1175/JCLI-D-24-0245.1, 2025.

Borella, A., Steer, C., Bellouin, N., and Boucher, O.: Concept of risk-aware contrail avoidance strategies, https://doi.org/10.5194/jecats-2026-2, 2026.

Boucher, O. and Reddy, M.: Climate trade-off between black carbon and carbon dioxide emissions, Energy Policy, 36, 193–200, https://doi.org/10.1016/j.enpol.2007.08.039, 2008.

Castino, F., Yin, F., Grewe, V., Soler, M., Simorgh, A., Yamashita, H., Matthes, S., Baumann, S., Dietmüller, S., and Linke, F.: Seasonal Variability of Aircraft Trajectories reducing NOx-climate Impacts under a Multitude of Weather Patterns, https://elib.dlr.de/185606/1/Castino_etal_sids_2021_paper_81.pdf, 2021.

Castino, F., Yin, F., Grewe, V., Yamashita, H., Matthes, S., Dietmüller, S., Baumann, S., Soler, M., Simorgh, A., Mendiguchia Meuser, M., Linke, F., and Lührs, B.: Decision-making strategies implemented in SolFinder 1.0 to identify eco-efficient aircraft trajectories: application study in AirTraf 3.0, Geoscientific Model Development, 17, 4031–4052, https://doi.org/10.5194/gmd-17-4031-2024, 2024.

Copernicus Climate Change Service: ERA5 hourly data on pressure levels from 1940 to present, https://doi.org/10.24381/CDS.BD0915C6, 2018a.

Copernicus Climate Change Service: ERA5 hourly data on single levels from 1940 to present, https://doi.org/10.24381/CDS.ADBB2D47, 2018b.

Dahlmann, K., Grewe, V., Frömming, C., and Burkhardt, U.: Can we reliably assess climate mitigation options for air traffic scenarios despite large uncertainties in atmospheric processes?, Transportation Research Part D: Transport and Environment, 46, 40–55, https://doi.org/10.1016/j.trd.2016.03.006, 2016.

Dahlmann, K., Matthes, S., and Grewe, V.: Conversion of climate metrics for policy applications, https://doi.org/10.5281/ZENODO.16355781, preprint, 2025.

Dean, T. R., Abbott, T. H., Engberg, Z., Masson, N., Teoh, R., Itcovitz, J. P., Stettler, M. E. J., and Shapiro, M. L.: Impact of forecast stability on navigational contrail avoidance, Environmental Research: Infrastructure and Sustainability, 5, 045 008, https://doi.org/10.1088/2634-4505/ae1da5, 2025.

DHCP: DelftBlue Supercomputer (Phase 2), https://www.tudelft.nl/dhpc/ark:/44463/DelftBluePhase2, delft High Performance Computing Centre (DHPC), 2024.

Dietmüller, S., Matthes, S., Dahlmann, K., Yamashita, H., Simorgh, A., Soler, M., Linke, F., Lührs, B., Meuser, M. M., Weder, C., Grewe, V., Yin, F., and Castino, F.: A Python library for computing individual and merged non-CO_2 algorithmic climate change functions: CLIMaCCF V1.0, Geoscientific Model Development, 16, 4405–4425, https://doi.org/10.5194/gmd-16-4405-2023, 2023.

https://doi.org/10.5194/jecats-2026-13
Preprint. Discussion started: 28 July 2026
© Author(s) 2026. CC BY 4.0 License.

Dischl, R., Sauer, D., Voigt, C., Harlaß, T., Sakellariou, F., Märkl, R., Schumann, U., Scheibe, M., Kaufmann, S., Roiger, A., Dörnbrack, A., Renard, C., Gauthier, M., Swann, P., Madden, P., Luff, D., Johnson, M., Ahrens, D., Sallinen, R., Schripp, T., Eckel, G., Bauder, U., and Le Clercq, P.: Measurements of particle emissions of an A350-941 burning 100 % sustainable aviation fuels in cruise, Atmospheric Chemistry and Physics, 24, 11 255–11 273, https://doi.org/10.5194/acp-24-11255-2024, 2024.

DuBois, D. and Paynter, G. C.: "Fuel Flow Method2" for Estimating Aircraft Emissions, SAE Transactions, 115, 1–14, http://www.jstor.org/stable/44657657, 2006.

EASA: ICAO Aircraft Engine Emissions Databank, https://www.easa.europa.eu/en/domains/environment/icao-aircraft-engine-emissions-databank, european Union Aviation Safety Agency, 2025.

ECMWF: IFS High-Resolution Operational Forecasts (HRES), https://www.ecmwf.int/en/forecasts/datasets/set-i, 2024.

Eichinger, R., Dahlmann, K., Grewe, V., Matthes, S., Niklaß, M., Lau, A., Zengerling, Z., Dietmüller, S., Völk, S., Megill, L., Voigt, C., Piontek, D., Kirschler, S., Plohr, M., Beckmann, B.-R., Schlemmer, L., Hanst, M., Köhler, C., Hollborn, S., Seifert, A., and Fundel, F.: Reference set of technical specifications for the MRV, Tech. rep., Deutsches Zentrum für Luft- und Raumfahrt (DLR), Deutscher Wetterdienst (DWD), 2025.

Engberg, Z., Teoh, R., Abbott, T., Dean, T., Stettler, M. E. J., and Shapiro, M. L.: Forecasting contrail climate forcing for flight planning and air traffic management applications: the CocipGrid model in pycontrails 0.51.0, Geoscientific Model Development, 18, 253–286, https://doi.org/10.5194/gmd-18-253-2025, 2025.

EUROCONTROL: User Manual for the Base of Aircraft Data (BADA) Revision 3.16, EIH Technical/Scientific Report No. 22/05/12-45, EUROCONTROL Experimental Centre (EEC), https://www.eurocontrol.int/model/bada (Accessed 2025-07-24), 2022.

European Commission: MRV non-CO2 data collection Guidance, Tech. rep., European Commission, eU Monitoring and reporting regulation (Implementing Regulation (EU) 2018/2066), 2026.

Frömming, C., Ponater, M., Dahlmann, K., Grewe, V., Lee, D. S., and Sausen, R.: Aviation-induced radiative forcing and surface temperature change in dependency of the emission altitude, Journal of Geophysical Research: Atmospheres, 117, 2012JD018 204, https://doi.org/10.1029/2012JD018204, 2012.

Frömming, C., Grewe, V., Brinkop, S., Jöckel, P., Haslerud, A. S., Rosanka, S., Van Manen, J., and Matthes, S.: Influence of weather situation on non-CO_2 aviation climate effects: the REACT4C climate change functions, Atmospheric Chemistry and Physics, 21, 9151–9172, https://doi.org/10.5194/acp-21-9151-2021, 2021.

Frömming, C., Grewe, V., Matthes, S., Dietmüller, S., Peter, P., Dahlmann, K., and Jöckel, P.: Expanding spatial and temporal coverage of climate change functions: Assessment and comparison with aCCFs, https://doi.org/10.5194/jecats-2026-7, 2026.

Gaillot, T., Beauchet, S., Lorne, D., and Krim, L.: The impact of fossil jet fuel emissions at altitude on climate change: A life cycle assessment study of a long-haul flight at different time horizons, Atmospheric Environment, 311, 119 983, https://doi.org/10.1016/j.atmosenv.2023.119983, 2023.

Gierens, K. M.: Exchange rates, trade-offs and risks in mitigation options for aviation, https://doi.org/10.5194/jecats-2026-8, 2026.

Grewe, V. and Stenke, A.: AirClim: an efficient tool for climate evaluation of aircraft technology, Atmospheric Chemistry and Physics, 8, 4621–4639, https://doi.org/10.5194/acp-8-4621-2008, 2008.

Grewe, V., Champougny, T., Matthes, S., Frömming, C., Brinkop, S., Søvde, O. A., Irvine, E. A., and Halscheidt, L.: Reduction of the air traffic's contribution to climate change: A REACT4C case study, Atmospheric Environment, 94, 616–625, https://doi.org/10.1016/j.atmosenv.2014.05.059, 2014a.

https://doi.org/10.5194/jecats-2026-13
Preprint. Discussion started: 28 July 2026
© Author(s) 2026. CC BY 4.0 License.

Grewe, V., Frömming, C., Matthes, S., Brinkop, S., Ponater, M., Dietmüller, S., Jöckel, P., Garny, H., Tsati, E., Dahlmann, K., Søvde, O. A., Fuglestvedt, J., Berntsen, T. K., Shine, K. P., Irvine, E. A., Champougny, T., and Hullah, P.: Aircraft routing with minimal climate impact: the REACT4C climate cost function modelling approach (V1.0), Geoscientific Model Development, 7, 175–201, https://doi.org/10.5194/gmd-7-175-2014, 2014b.

Grewe, V., Matthes, S., Frömming, C., Brinkop, S., Jöckel, P., Gierens, K., Champougny, T., Fuglestvedt, J., Haslerud, A., Irvine, E., and Shine, K.: Feasibility of climate-optimized air traffic routing for trans-Atlantic flights, Environmental Research Letters, 12, 034 003, https://doi.org/10.1088/1748-9326/aa5ba0, 2017.

Grewe, V., Matthes, S., and Dahlmann, K.: The contribution of aviation NO_x emissions to climate change: are we ignoring methodological flaws?, Environmental Research Letters, 14, 121 003, https://doi.org/10.1088/1748-9326/ab5dd7, 2019.

Grewe, V., Niklaß, M., Dahlmann, K., Eichinger, R., Matthes, S., Lau, A., Scheelhaase, J., Linke, F., and Plohr, M.: Pathways for including non-carbon dioxide aviation climate effects in the European Emission Trading System, Communications Earth & Environment, 7, 243, https://doi.org/10.1038/s43247-026-03265-w, 2026.

Harlass, T., Dischl, R., Kaufmann, S., Märkl, R., Sauer, D., Scheibe, M., Stock, P., Bräuer, T., Dörnbrack, A., Roiger, A., Schlager, H., Schumann, U., Pühl, M., Schripp, T., Grein, T., Bondorf, L., Renard, C., Gauthier, M., Johnson, M., Luff, D., Madden, P., Swann, P., Ahrens, D., Sallinen, R., and Voigt, C.: Measurement report: In-flight and ground-based measurements of nitrogen oxide emissions from latest-generation jet engines and 100 % sustainable aviation fuel, Atmospheric Chemistry and Physics, 24, 11 807–11 822, https://doi.org/10.5194/acp-24-11807-2024, 2024.

Hoffmann, L. and Spang, R.: Reanalysis tropopause data repository, https://doi.org/10.26165/JUELICH-DATA/UBNGI2, 2021.

ICAO: Airport Air Quality Manual, Tech. Rep. Doc 9889, International Civil Aviation Organization (ICAO), Montréal, Canada, ISBN 978-92-9231-862-8, 2016.

ICAO: ICAO Carbon Emissions Calculator Methodology version 11, 2018.

IPCC: Aviation and the Global Atmosphere, Tech. rep., Cambridge University Press, (eds Penner, J. E., et al.), 1999.

Irvine, E. A., Hoskins, B. J., Shine, K. P., Lunnon, R. W., and Froemming, C.: Characterizing North Atlantic weather patterns for climate-optimal aircraft routing, Meteorological Applications, 20, 80–93, https://doi.org/10.1002/met.1291, 2013.

Jaramillo, P., Kahn Ribeiro, S., Newman, P., Dhar, S., Diemuodeke, O., Kajino, T., Lee, D., Nugroho, S., Ou, X., Hammer Strømman, A., and Whitehead, J.: Transport, in: Climate change 2022: Mitigation of climate change. Contribution of working group III to the sixth assessment report of the intergovernmental panel on climate change, edited by Shukla, P., Skea, J., Slade, R., Khourdajie, A. A., van Diemen, R., McCollum, D., Pathak, M., Some, S., Vyas, P., Fradera, R., Belkacemi, M., Hasija, A., Lisboa, G., Luz, S., and Malley, J., Cambridge University Press, Cambridge, UK and New York, NY, USA, https://doi.org/10.1017/9781009157926.012, section: 10 Type: Book Section, 2022.

Jöckel, P., Kerkweg, A., Pozzer, A., Sander, R., Tost, H., Riede, H., Baumgaertner, A., Gromov, S., and Kern, B.: Development cycle 2 of the Modular Earth Submodel System (MESSy2), Geoscientific Model Development, 3, 717–752, https://doi.org/10.5194/gmd-3-717-2010, 2010.

Kirschler, S., Voigt, C., Piontek, D., Juchem, M., Widmaier, K., Wang, Z., Nalianda, D., Todt, C., Zengerling, Z., Solzer, J., Lau, A., Schumann, U., Bellouin, N., Stettler, M., and Teoh, R.: Towards climate compatible aviation: operational feasibility of contrail avoidance by flight path adjustments, https://doi.org/10.21203/rs.3.rs-8799231/v1, 2026.

https://doi.org/10.5194/jecats-2026-13
Preprint. Discussion started: 28 July 2026
© Author(s) 2026. CC BY 4.0 License.

Köhler, M. O., Rädel, G., Dessens, O., Shine, K. P., Rogers, H. L., Wild, O., and Pyle, J. A.: Impact of perturbations to nitrogen oxide emissions from global aviation, Journal of Geophysical Research: Atmospheres, 113, 2007JD009 140, https://doi.org/10.1029/2007JD009140, 2008.

Lee, D. S., Fahey, D. W., Skowron, A., Allen, M. R., Burkhardt, U., Chen, Q., Doherty, S. J., Freeman, S., Forster, P. M., and Fuglestvedt, J.: The contribution of global aviation to anthropogenic climate forcing for 2000 to 2018, Atmospheric Environment, 244, 117 834, https://doi.org/10.1016/j.atmosenv.2020.117834, 2021.

Lee, D. S., Allen, M. R., Cumpsty, N., Owen, B., Shine, K. P., and Skowron, A.: Uncertainties in mitigating aviation non-CO_2 emissions for climate and air quality using hydrocarbon fuels, Environmental Science: Atmospheres, 3, 1693–1740, https://doi.org/10.1039/D3EA00091E, 2023.

Low, J., Teoh, R., Ponsonby, J., Gryspeerdt, E., Shapiro, M., and Stettler, M. E. J.: Ground-based contrail observations: comparisons with reanalysis weather data and contrail model simulations, Atmospheric Measurement Techniques, 18, 37–56, https://doi.org/10.5194/amt-18-37-2025, 2025.

Lührs, B., Linke, F., Matthes, S., Grewe, V., and Yin, F.: Climate Impact Mitigation Potential of European Air Traffic in a Weather Situation with Strong Contrail Formation, Aerospace, 8, 50, https://doi.org/10.3390/aerospace8020050, 2021.

Martin Frias, A., Shapiro, M. L., Engberg, Z., Zopp, R., Soler, M., and Stettler, M. E. J.: Feasibility of contrail avoidance in a commercial flight planning system: an operational analysis, Environmental Research: Infrastructure and Sustainability, 4, 015 013, https://doi.org/10.1088/2634-4505/ad310c, 2024.

Maruhashi, J., Grewe, V., Frömming, C., Jöckel, P., and Dedoussi, I. C.: Transport patterns of global aviation NO_x and their short-term O_3 radiative forcing – a machine learning approach, Atmospheric Chemistry and Physics, 22, 14 253–14 282, https://doi.org/10.5194/acp-22-14253-2022, 2022.

Maruhashi, J., Mertens, M., Grewe, V., and Dedoussi, I. C.: A multi-method assessment of the regional sensitivities between flight altitude and short-term O_3 climate warming from aircraft NO_x emissions, Environmental Research Letters, 19, 054 007, https://doi.org/10.1088/1748-9326/ad376a, 2024.

Matthes, S., Schumann, U., Grewe, V., Frömming, C., Dahlmann, K., Koch, A., and Mannstein, H.: Climate Optimized Air Transport, in: Atmospheric Physics, pp. 727–746, Springer Berlin Heidelberg, Berlin, Heidelberg, ISBN 978-3-642-30182-7 978-3-642-30183-4, https://doi.org/10.1007/978-3-642-30183-4_44, series Title: Research Topics in Aerospace, 2012.

Matthes, S., Lührs, B., Dahlmann, K., Grewe, V., Linke, F., Yin, F., Klingaman, E., and Shine, K. P.: Climate-Optimized Trajectories and Robust Mitigation Potential: Flying ATM4E, Aerospace, 7, 156, https://doi.org/10.3390/aerospace7110156, 2020.

Matthes, S., Lim, L., Burkhardt, U., Dahlmann, K., Dietmüller, S., Grewe, V., Haslerud, A. S., Hendricks, J., Owen, B., Pitari, G., Righi, M., and Skowron, A.: Mitigation of Non-CO2 Aviation's Climate Impact by Changing Cruise Altitudes, Aerospace, 8, 36, https://doi.org/10.3390/aerospace8020036, 2021.

Matthes, S., Dietmüller, S., Dahlmann, K., Frömming, C., Peter, P., Yamashita, H., Grewe, V., Yin, F., and Castino, F.: Updated algorithmic climate change functions (aCCF) V1.0A: Evaluation with the climate-response model AirClim V2.0, https://doi.org/10.5194/gmd-2023-92, preprint, 2023.

Megill, L., Deck, K., and Grewe, V.: Alternative climate metrics to the Global Warming Potential are more suitable for assessing aviation non-CO2 effects, Communications Earth & Environment, 5, 249, https://doi.org/10.1038/s43247-024-01423-6, 2024.

Myhre, G., Nilsen, J. S., Gulstad, L., Shine, K. P., Rognerud, B., and Isaksen, I. S. A.: Radiative forcing due to stratospheric water vapour from CH_4 oxidation, Geophysical Research Letters, 34, 2006GL027 472, https://doi.org/10.1029/2006GL027472, 2007.

https://doi.org/10.5194/jecats-2026-13
Preprint. Discussion started: 28 July 2026
© Author(s) 2026. CC BY 4.0 License.

Märkl, R. S., Voigt, C., Sauer, D., Dischl, R. K., Kaufmann, S., Harlaß, T., Hahn, V., Roiger, A., Weiß-Rehm, C., Burkhardt, U., Schumann, U., Marsing, A., Scheibe, M., Dörnbrack, A., Renard, C., Gauthier, M., Swann, P., Madden, P., Luff, D., Sallinen, R., Schripp, T., and Le Clercq, P.: Powering aircraft with 100 % sustainable aviation fuel reduces ice crystals in contrails, Atmospheric Chemistry and Physics, 24, 3813–3837, https://doi.org/10.5194/acp-24-3813-2024, 2024.

Nuic, A., Poles, D., and Mouillet, V.: BADA: An advanced aircraft performance model for present and future ATM systems, International Journal of Adaptive Control and Signal Processing, 24, 850–866, https://doi.org/10.1002/acs.1176, 2010.

Piontek, D., Widmaier, K., Kirschler, S., Clément, J., Edeline, J., Smretschnig, J., Antonello, D., Philak, T., Dietmuller, S., Matthes, S., Dahlmann, K., Yin, F., and Voigt, C.: Towards The Implementation of Climate-Optimized Air Traffic in Northern Europe: Feasibility and Airspace Constraints of Pre-Tactical Contrail Mitigation, https://doi.org/https://dx.doi.org/10.2139/ssrn.6959658, preprint, 2026.

Ponater, M.: Distinctive efficacies of the components contributing to total aviation climate impact, in: Proceedings of the 2nd international conference on transport, atmosphere and climate (TAC-2), edited by Sausen, R., van Velthoven, P., Brüning, C., and Blum, A., vol. 2010 of *Forschungsbericht*, pp. 227–232, Deutsches Zentrum für Luft- und Raumfahrt, https://elib.dlr.de/65284/, number: 10, 2010.

Prather, M. J., Gettelman, A., and Penner, J. E.: Trade-offs in aviation impacts on climate favour non-CO2 mitigation, Nature, 643, 988–993, https://doi.org/10.1038/s41586-025-09198-2, 2025.

Rao, P., Yin, F., Grewe, V., Yamashita, H., Jöckel, P., Matthes, S., Mertens, M., and Frömming, C.: Case Study for Testing the Validity of NOx-Ozone Algorithmic Climate Change Functions for Optimising Flight Trajectories, Aerospace, 9, 231, https://doi.org/10.3390/aerospace9050231, 2022.

Rao, P., Dwight, R., Singh, D., Maruhashi, J., Dedoussi, I., Grewe, V., and Frömming, C.: The ozone radiative forcing of nitrogen oxide emissions from aviation can be estimated using a probabilistic approach, Communications Earth & Environment, 5, 558, https://doi.org/10.1038/s43247-024-01691-2, 2024.

Rogowski, M., Aseeri, S., Keyes, D., and Dalcin, L.: mpi4py.futures: MPI-Based Asynchronous Task Execution for Python, IEEE Transactions on Parallel and Distributed Systems, 34, 611–622, https://doi.org/10.1109/TPDS.2022.3225481, 2023.

Rosanka, S., Frömming, C., and Grewe, V.: The impact of weather patterns and related transport processes on aviation's contribution to ozone and methane concentrations from NO_x emissions, Atmospheric Chemistry and Physics, 20, 12 347–12 361, https://doi.org/10.5194/acp-20-12347-2020, 2020.

Rosenow, J., Förster, S., Lindner, M., and Fricke, H.: Multicriteria-Optimized Trajectories Impacting Today's Air Traffic Density, Efficiency, and Environmental Compatibility, Journal of Air Transportation, 27, 8–15, https://doi.org/10.2514/1.D0086, 2019.

Sausen, R. and Schumann, U.: Estimates of the Climate Response to Aircraft CO2 and NO x Emissions Scenarios, Climatic Change, 44, 27–58, https://doi.org/10.1023/A:1005579306109, 2000.

Sausen, R., Hofer, S., Gierens, K., Bugliaro, L., Ehrmanntraut, R., Sitova, I., Walczak, K., Burridge-Diesing, A., Bowman, M., and Miller, N.: Can we successfully avoid persistent contrails by small altitude adjustments of flights in the real world?, Meteorologische Zeitschrift, 33, 83–98, https://doi.org/10.1127/metz/2023/1157, 2024.

Schumann, U.: On conditions for contrail formation from aircraft exhausts, Meteorologische Zeitschrift, 5, 4–23, https://doi.org/10.1127/metz/5/1996/4, 1996.

Schumann, U., Mayer, B., Graf, K., and Mannstein, H.: A Parametric Radiative Forcing Model for Contrail Cirrus, Journal of Applied Meteorology and Climatology, 51, 1391–1406, https://doi.org/10.1175/JAMC-D-11-0242.1, 2012.

https://doi.org/10.5194/jecats-2026-13
Preprint. Discussion started: 28 July 2026
© Author(s) 2026. CC BY 4.0 License.

Schumann, U., Baumann, R., Baumgardner, D., Bedka, S. T., Duda, D. P., Freudenthaler, V., Gayet, J.-F., Heymsfield, A. J., Minnis, P., Quante, M., Raschke, E., Schlager, H., Vázquez-Navarro, M., Voigt, C., and Wang, Z.: Properties of individual contrails: a compilation of observations and some comparisons, Atmospheric Chemistry and Physics, 17, 403–438, https://doi.org/10.5194/acp-17-403-2017, 2017.

Shapiro, M., Engberg, Z., Teoh, R., Stettler, M., Dean, T., and Abbott, T.: pycontrails: Python library for modeling aviation climate impacts, https://doi.org/10.5281/zenodo.16575452, 2025.

Simorgh, A. and Soler, M.: Climate-optimized flight planning can effectively reduce the environmental footprint of aviation in Europe at low operational costs, Communications Earth & Environment, 6, 66, https://doi.org/10.1038/s43247-025-02031-8, 2025.

Simorgh, A., Soler, M., González-Arribas, D., Matthes, S., Grewe, V., Dietmüller, S., Baumann, S., Yamashita, H., Yin, F., Castino, F., Linke, F., Lührs, B., and Meuser, M. M.: A Comprehensive Survey on Climate Optimal Aircraft Trajectory Planning, Aerospace, 9, 146, https://doi.org/10.3390/aerospace9030146, 2022.

Smith, J. R., Grobler, C., Hodgson, P. J., Mukhopadhaya, J., Shapiro, M. L., Mirolo, M., Stettler, M. E. J., Eastham, S. D., and Barrett, S. R. H.: The climate opportunities and risks of contrail avoidance, Nature Communications, 17, 2092, https://doi.org/10.1038/s41467-026-68784-8, 2026.

Stevenson, D. S., Doherty, R. M., Sanderson, M. G., Collins, W. J., Johnson, C. E., and Derwent, R. G.: Radiative forcing from aircraft NO_x emissions: Mechanisms and seasonal dependence, Journal of Geophysical Research: Atmospheres, 109, 2004JD004 759, https://doi.org/10.1029/2004JD004759, 2004.

Szopa, S., Naik, V., Adhikary, B., Artaxo, P., Berntsen, T., Collins, W., Fuzzi, S., Gallardo, L., Kiendler-Scharr, A., Klimont, Z., Liao, H., Unger, N., and Zanis, P.: Short-lived climate forcers, in: Climate change 2021: The physical science basis. Contribution of working group I to the sixth assessment report of the intergovernmental panel on climate change, edited by Masson-Delmotte, V., Zhai, P., Pirani, A., Connors, S. L., Péan, C., Berger, S., Caud, N., Chen, Y., Goldfarb, L., Gomis, M. I., Huang, M., Leitzell, K., Lonnoy, E., Matthews, J. B. R., Maycock, T. K., Waterfield, T., Yelekçi, O., Yu, R., and Zhou, B., pp. 817–921, Cambridge University Press, Cambridge, UK and New York, NY, USA, https://doi.org/10.1017/9781009157896.008, section: 6 Type: Book Section, 2021.

Søvde, O. A., Matthes, S., Skowron, A., Iachetti, D., Lim, L., Owen, B., Hodnebrog, , Di Genova, G., Pitari, G., Lee, D. S., Myhre, G., and Isaksen, I. S.: Aircraft emission mitigation by changing route altitude: A multi-model estimate of aircraft NOx emission impact on O3 photochemistry, Atmospheric Environment, 95, 468–479, https://doi.org/10.1016/j.atmosenv.2014.06.049, 2014.

Teoh, R., Schumann, U., Majumdar, A., and Stettler, M. E. J.: Mitigating the Climate Forcing of Aircraft Contrails by Small-Scale Diversions and Technology Adoption, Environmental Science & Technology, 54, 2941–2950, https://doi.org/10.1021/acs.est.9b05608, 2020.

Teoh, R., Schumann, U., Gryspeerdt, E., Shapiro, M., Molloy, J., Koudis, G., Voigt, C., and Stettler, M.: Aviation contrail climate effects in the North Atlantic from 2016–2021, Atmospheric Chemistry and Physics, 22, 10 919–10 935, https://doi.org/10.5194/acp-22-10919-2022, 2022.

Teoh, R., Engberg, Z., Schumann, U., Voigt, C., Shapiro, M., Rohs, S., and Stettler, M. E. J.: Global aviation contrail climate effects from 2019 to 2021, Atmospheric Chemistry and Physics, 24, 6071–6093, https://doi.org/10.5194/acp-24-6071-2024, 2024a.

Teoh, R., Engberg, Z., Shapiro, M., Dray, L., and Stettler, M. E. J.: The high-resolution Global Aviation emissions Inventory based on ADS-B (GAIA) for 2019–2021, Atmospheric Chemistry and Physics, 24, 725–744, https://doi.org/10.5194/acp-24-725-2024, 2024b.

Van Manen, J. and Grewe, V.: Algorithmic climate change functions for the use in eco-efficient flight planning, Transportation Research Part D: Transport and Environment, 67, 388–405, https://doi.org/10.1016/j.trd.2018.12.016, 2019.

Voigt, C., Lelieveld, J., Schlager, H., Schneider, J., Curtius, J., Meerkötter, R., Sauer, D., Bugliaro, L., Bohn, B., Crowley, J. N., Erbertseder, T., Groß, S., Hahn, V., Li, Q., Mertens, M., Pöhlker, M. L., Pozzer, A., Schumann, U., Tomsche, L., Williams, J., Zahn, A., Andreae, M.,

https://doi.org/10.5194/jecats-2026-13
Preprint. Discussion started: 28 July 2026
© Author(s) 2026. CC BY 4.0 License.

Borrmann, S., Bräuer, T., Dörich, R., Dörnbrack, A., Edtbauer, A., Ernle, L., Fischer, H., Giez, A., Granzin, M., Grewe, V., Harder, H., Heinritzi, M., Holanda, B. A., Jöckel, P., Kaiser, K., Krüger, O. O., Lucke, J., Marsing, A., Martin, A., Matthes, S., Pöhlker, C., Pöschl, U., Reifenberg, S., Ringsdorf, A., Scheibe, M., Tadic, I., Zauner-Wieczorek, M., Henke, R., and Rapp, M.: Cleaner Skies during the COVID-19 Lockdown, Bulletin of the American Meteorological Society, 103, E1796–E1827, https://doi.org/10.1175/BAMS-D-21-0012.1, 2022.

Voigt, C., Märkl, R., Sauer, D., Dischl, R., Kaufmann, S., Bräuer, T., Jurkat, T., Renard, C., Seeliger, K., Chenadec, G. L., Moreau, J., Yu, F., Bonne, N., Roche, A., Zelina, J., Dörnbrack, A., Eirenschmalz, L., Heckl, C., Horst, E., Lichtenstern, M., Marsing, A., Roiger, A., Scheibe, M., Stock, P., Giez, A., Eckel, G., Neumann, G., Vals, M., Requena-Esteban, E., and Clercq, P. L.: Substantial aircraft contrail formation at low soot emission levels, https://doi.org/10.21203/rs.3.rs-6559440/v1, 2025.

Wilcox, L., Shine, K., and Hoskins, B.: Radiative forcing due to aviation water vapour emissions, Atmospheric Environment, 63, 1–13, https://doi.org/10.1016/j.atmosenv.2012.08.072, 2012.

Wilhelm, L., Gierens, K., and Rohs, S.: Weather Variability Induced Uncertainty of Contrail Radiative Forcing, Aerospace, 8, 332, https://doi.org/10.3390/aerospace8110332, 2021.

Yamashita, H., Yin, F., Grewe, V., Jöckel, P., Matthes, S., Kern, B., Dahlmann, K., and Frömming, C.: Newly developed aircraft routing options for air traffic simulation in the chemistry–climate model EMAC 2.53: AirTraf 2.0, Geoscientific Model Development, 13, 4869–4890, https://doi.org/10.5194/gmd-13-4869-2020, 2020.

Yin, F., Grewe, V., Frömming, C., and Yamashita, H.: Impact on flight trajectory characteristics when avoiding the formation of persistent contrails for transatlantic flights, Transportation Research Part D: Transport and Environment, 65, 466–484, https://doi.org/10.1016/j.trd.2018.09.017, 2018a.

Yin, F., Grewe, V., van Manen, J., Matthes, S., Yamashita, H., Linke, F., and Lührs, B.: Verification of the ozone algorithmic climate change functions for predicting the short-term NOx effects from aviation en-route, in: Proceedings of the International Conference on Research in Air Transportation (ICRAT), Barcelona, Spain, 2018b.

Yin, F., Grewe, V., Castino, F., Rao, P., Matthes, S., Dahlmann, K., Dietmüller, S., Frömming, C., Yamashita, H., and Peter, P.: Predicting the climate impact of aviation for en-route emissions: the algorithmic climate change function submodel ACCF 1.0 of EMAC 2.53, Geoscientific Model Development, 16, 3313–3334, https://doi.org/10.5194/gmd-16-3313-2023, 2023.

Yu, F., Kärcher, B., and Anderson, B. E.: Revisiting Contrail Ice Formation: Impact of Primary Soot Particle Sizes and Contribution of Volatile Particles, Environmental Science & Technology, 58, 17 650–17 660, https://doi.org/10.1021/acs.est.4c04340, 2024.

Zengerling, Z. L., Linke, F., Weder, C. M., Dietmüller, S., Matthes, S., and Peter, P.: Flying low and slow: Application of algorithmic climate change functions to assess the climate mitigation potential of reduced cruise altitudes and speeds on different days, Meteorologische Zeitschrift, 33, 67–81, https://doi.org/10.1127/metz/2023/1194, 2023.